JAIST Repository
https://dspace.jaist.ac.jp/

Title	Interim Report of Detailed Coding/Decoding Algorithms and Correlation Estimation Techniques
Author(s)	Anwar, Khoirul; He, Xin; Hou, Jiancao; Komulainen, Petri; Matsumoto, Tad; Matth´e, Maximilian; Wolf, Albrecht; Yi, Na; Zhou, Xiaobo
Citation	ICT-619555 RESCUE D2.1.1 Version 1.0: 1-54
Issue Date	2014-10
Type	Research Paper
Text version	publisher
URL	http://hdl.handle.net/10119/13796
Rights	This material is posted here by permission of the EU FP7 RESCUE Project. http://www.ict-rescue.eu/ RESCUE is founded by the European Commission under the 7th Framework Programme,Theme 3-"ICT"call FP7-ICT-2013-11,Work Programme Topic 1.1"Future Networks"
Description	

JAIST
JAPAN
ADVANCED INSTITUTE OF
SCIENCE AND TECHNOLOGY

Japan Advanced Institute of Science and Technology

ICT-619555 RESCUE

D2.1.1 Version 1.0

Interim Report of Detailed Coding/Decoding Algorithms and Correlation Estimation Techniques

Contractual Date of Delivery to the CEC:	10/2014
Actual Date of Delivery to the CEC:	10/2014
Editor:	Petri Komulainen
Authors:	Khoirul Anwar, Xin He, Jiancao Hou, Petri Komulainen, Tad Matsumoto, Maximilian Matthé, Albrecht Wolf, Na Yi, Xiaobo Zhou
Participants:	JAIST, TUD, UNIS, UOULU
Work package:	WP2 – Code and algorithm design and optimization
Security:	**PU**
Nature:	**R**
Version:	1.0
Total number of pages:	54

Abstract: The RESCUE project proposes a novel multi-route communication technology design targeted for multi-hop networks, based on cooperative decode-and-forward (DF) relaying allowing intra-link errors and utilizing distributed turbo codes. This deliverable provides initial results and descriptions of the considered coding/decoding and correlation estimation algorithms. The state-of-the-art in simple relay network models is summarized, and new source-correlation estimation methods and signaling protocols are proposed. According to the numerical results, the decoding performance is close to the theoretical limit when the correlation is known. Furthermore, more general system models are considered, including non-orthogonal multiple access, multi-hop communication where the destination is more than two hops away from the source, and multiple-access relaying where two sources utilize a single relay node. In order to support system level development and simulations, a new simulation abstraction concept is also proposed.

Keyword list: cooperative relaying, decode-and-forward, distributed turbo code, interleave division multiple access, iterative decoding, lossy forwarding, multi-hop communication, wireless networks

Disclaimer:

Executive Summary

The RESCUE project – "Links-on-the-fly Technology for Robust, Efficient, and Smart Communication in Unpredictable Environments" – proposes a novel multi-route communication technology design targeted for multi-hop networks that are subject to dynamic topology changes. This deliverable provides initial results and descriptions of the coding/decoding and source-correlation estimation algorithms considered in the project.

The RESCUE cooperative protocol consists of decode-and-forward (DF) or extract-and-forward (EF) relaying that allows intra-link errors, combined with distributed turbo coding that brings improved error protection. The relaying nodes decode, interleave, and re-encode the data, which causes no bandwidth expansion compared to the original signal. The possible decoding errors at the relaying nodes result in limited correlation between the forwarded packet copies. The destination combines the packet copies via iterative decoding, taking into account the correlations by properly weighting each copy. For the simple network model consisting of a single source, a set of parallel relay nodes, and one destination node, no major performance improvements by code design can be found since the performance of the state-of-the-art codes is already close to the theoretical limit when the correlation is known.

One of the main remaining challenges lies in how to obtain the knowledge of the correlation between the relayed data sequences to the destination. The decoding errors at relays result in bit-flipping between the original and forwarded sequences. Thus the correlation estimation is essentially bit error probability estimation. At the destination, the estimation is carried out along with the iterative decoding, and each received packet is treated separately. The estimation has three phases. First, the log-likelihood ratio (LLR) samples to be used for estimation are selected. Then, pairwise bit error rates (BERs) between transmitted packets are estimated. Finally, the pairwise BERs are used to resolve the actual transmitter-specific BERs. Several novel ideas to each phase are proposed that, compared to the state-of-the-art methods, result in improved decoding performance and/or reduced complexity. An alternative approach is to estimate the BER already at the relays and then forward the information to the destination. The estimate can be based on the signal-to-noise ratio (SNR) of the source-relay link. On the other hand, if a cyclic redundancy check (CRC) is available, it makes sense for the relays to check it in order to identify correctly decoded packets. It is a future design challenge to find a protocol that provides the best trade-off between decoding performance, estimation complexity, and signaling overhead.

More general system models and their coding/decoding challenges are also considered. First, non-orthogonal multiple access for the relay transmissions by employing interleave-division multiple access (IDMA) is proposed. The approach improves spectral efficiency if multi-user detection (MUD) at the destination is used. Then, a multiple-access relaying model where two sources utilize a single relay node and communicate to a common destination node is addressed. The relay applies network coding and transmits a single stream to aid the destination in recovering the two sources.

When the network model is extended to cover more than two hops between the source and the relay, and when there are multiple parallel relays at each stage, the decoding strategy at the relays needs to be designed. If complexity is not an issue, the relays may carry out the same type iterative multi-packet combining as the destination does. On the other hand, at the destination, the errors in the received packet copies may become correlated, when the same errors are transmitted by the parallel relays of the second stage. However, the cross-link problem does not seem to be severe, at least when the error probabilities remain relatively low.

In the system level, and for the higher layer functionalities such as multi-rate control, power control, automatic repeat request (ARQ) protocol, and medium access control (MAC), it is desirable to be able to run simulations without the need to implement all the details of the physical layer. To this end, a quality mapping that predicts the BER distribution at a receiver that combines multiple packet copies is also developed in this document.

Authors

Partner	Name	E-mail / Phone
Japan Advanced Institute of Science and Technology (JAIST)	Tad Matsumoto Khoirul Anwar	matumoto@jaist.ac.jp anwar-k@jaist.ac.jp
Technical University Dresden (TUD)	Maximilian Matthé Albrecht Wolf	maximilian.matthe@ifn.et.tu-dresden.de albrecht.wolf@ifn.et.tu-dresden.de
University of Surrey (UNIS)	Na Yi Jiancao Hou	n.yi@surrey.ac.uk jiancao.hou@surrey.ac.uk
University of Oulu (UOULU)	Petri Komulainen Xiaobo Zhou Xin He	petri.komulainen@ee.oulu.fi / +358 294 482971 xiaobo.zhou@ee.oulu.fi xin.he@ee.oulu.fi

Table of Contents

Executive Summary ... **2**

Authors ... **3**

Table of Contents ... **5**

List of Acronyms and Abbreviations ... **6**

1. Introduction ... **8**

2. Multi-route Relaying ... **10**

2.1 System Models and Theoretical Background ... 10
2.1.1 Single-Relay Model ... 10
2.1.2 CEO Relaying Model ... 11
2.2 Distributed Turbo Codes – Coding and Decoding ... 12
2.2.1 Single-Relay Model ... 12
2.2.2 CEO Relaying Model ... 14
2.2.2.1 Transmitter ... 14
2.2.2.2 Receiver ... 14
2.3 Numerical Results ... 16
2.3.1 Single-Relay Model ... 16
2.3.2 CEO Relaying Model ... 18

3. Source Correlation Estimation ... **20**

3.1 Source Correlation Estimation at the Destination ... 20
3.1.1 State-of-The-Art Algorithm and Performance ... 20
3.1.2 Modification of the SoTA Estimation Algorithms ... 22
3.1.2.1 Threshold Adaptation ... 22
3.1.2.2 Reducing Estimation Variance ... 22
3.1.3 Novel Approaches for Pairwise Estimators ... 24
3.1.3.1 Model-Based Unbiased Estimator ... 24
3.1.3.2 Heuristic Estimators ... 24
3.1.4 Numerical Results of Proposed Estimators ... 25
3.1.4.1 Reference Scenario and State-of-The-Art Performance ... 25
3.1.4.2 Performance of Modified Estimators ... 25
3.1.4.3 Performance of Novel Pairwise Estimators ... 28
3.2 Source Correlation Estimation at Relays ... 31
3.2.1 System Model ... 31
3.2.2 The Source-Relay (S-R) Correlation Knowledge Estimation ... 31
3.2.3 Performance Analysis ... 32
3.2.3.1 Convergence Property ... 32
3.2.3.2 BER Performance ... 33
3.2.4 Summary ... 34
3.3 Summary and Discussion ... 34

4. Advanced Topologies and Access Methods ... **36**

4.1 Interleave-Division Multiple-Access (IDMA) ... 36
4.1.1 Code design ... 36
4.1.2 Single-User Detection (SUD) ... 37
4.1.3 Multi-User Detection (MUD) ... 38

4.1.4 Numerical Results 39
4.2 Coding and Decoding for Multi-Hop Relaying 39
4.2.1 System Model: Coding and Decoding 40
4.2.2 Results and Discussion 41
4.3 Joint Adaptive Network and Channel Coding for Orthogonal Multiple Access Relay Channel 42
4.3.1 System Model 42
4.3.1.1 Network Correlation 43
4.3.2 Coding and Decoding Scheme 43
4.3.2.1 Coding Structure at The Source and Relay Nodes 43
4.3.2.2 Joint Network-Channel Decoding Structure 44
4.3.3 Numerical Results 45

5. Support for System Design 47

5.1 Multi-Rate Coding 47
5.2 Interaction with Higher Layers 48
5.2.1 Functional Block Diagram and Interfaces 48
5.2.2 Simulation Abstraction for Higher Layers 49

6. Conclusion 51

7. References 52

List of Acronyms and Abbreviations

Term	Description
ACC	Accumulator
AF	Amplify-and-Forward
ARQ	Automatic Repeat Request
AWGN	Additive White Gaussian Noise
BER	Bit Error Rate
BLER	Block Error Rate
BPSK	Binary Phase-Shift Keying
BSC	Binary Symmetric Channel
CDMA	Code-Division Multiple Access
CEO	Chief Executive Officer
CF	Compress-and-Forward
CI	Confidence Indicator
CRC	Cyclic Redundancy Check
CSI	Channel State Information
DACC	Doped Accumulator
DF	Decode-and-Forward
EBSA	EXIT-Constrained Binary Switching Algorithm
EESM	Exponential Effective SNR Mapping
EM	Extended Mapping
EF	Extract-and-Forward
EXIT	Extrinsic Information Transfer Chart
FC	Fusion Center
FEC	Forward Error Correction
FER	Frame Error Rate
GI	Global Iteration
IDMA	Interleave-Division Multiple Access
IL	Interleaver
LI	Local Iteration
LLR	Log-Likelihood Ratio
LTE	Long-Term Evolution
MA	Multiple Access
MAC	Multiple Access Channel
MAC	Medium Access Control
MAI	Multiple Access Interference
MAP	Maximum a Posteriori
MARC	Multiple Access Relay Channel
MARC-IE	Multiple Access Relay Channel allowing Intra-link Errors
MI	Mutual Information
MCS	Modulation and Coding Set
MSE	Mean Squared Error
MUD	Multi-User Detection
OFDM	Orthogonal Frequency-Division Multiplexing
P2P	Point-to-Point
PCCC	Parallel Concatenated Convolutional Codes
PHY	Physical Layer
QAM	Quadrature Amplitude Modulation
QPSK	Quadrature Phase-Shift Keying
RESCUE	Links-on-the-fly Technology for Robust, Efficient, and Smart Communication in Unpredictable Environments
S-DF	Selective Decode-and-Forward
SDR	Software-Defined Radio
SINR	Signal-to-Interference+Noise Ratio

SNR	Signal-to-Noise Ratio
SoTA	State-of-The-Art
SPC	Single-Parity Check
SPC-IrR	Single-Parity Check and Irregular Repetition
S-R	Source-Relay
SUD	Single-User Detection
V2V	Vehicle-to-Vehicle
WP	Work Package
WSN	Wireless Sensor Network

1. Introduction

The RESCUE project – "Links-on-the-fly Technology for Robust, Efficient, and Smart Communication in Unpredictable Environments" – aims to bring forth a novel communication technology design targeted for largely unplanned multi-hop networks that are further subject to dynamic topology changes. The potential system scenarios for the links-on-the-fly concept have been described in D1.1 [D11]. The first scenario is public safety operations that take place in areas where the communication infrastructure is partially inoperable due to a disaster such as an earthquake. The second scenario is vehicle-to-vehicle (V2V) communication, where cars and other vehicles share, for example, safety-critical information about the road and traffic conditions with each other. The identified communication applications range from video streaming and text messaging to group communication (push-to-talk), automatic vehicle/person location, and cooperative collision warning. D1.1 also lists the identified key functional requirements and design challenges for different protocol layers, from the physical to the network layer.

The RESCUE cooperative protocol consists of decode-and-forward (DF) relaying that allows intra-link errors, combined with distributed turbo coding that brings improved error protection. The relaying nodes decode and re-encode the data, which causes no bandwidth expansion compared to the original signal. The possible decoding errors at the relaying nodes result in limited correlation between the forwarded packet copies that the destination takes into account when decoding. The basic principles of the RESCUE relaying strategy have been presented in [AM12a; ZHA+12; ZCA+12]. The main sources of performance gains in terms of spectral efficiency, transmit power, and outage probability obtained by the links-on-the-fly technology are:

- Route diversity: The signal is relayed via multiple (possibly unreliable) disjoint routes and combined at the destination. Thus, the probability of successful reception increases.

- Utilizing the broadcast nature of radio transmission: Multiple relay nodes capture the original transmission, and thus more of the received signal energy is exploited.

- Lossy forwarding: The relay nodes allow decoding errors, and thus a higher number of relays are able to assist. Also, a higher portion of the received signal energy is thus exploited.

- Distributed turbo codes and iterative decoding: The parallel relays form together a very powerful low-rate forward error correction (FEC) code, which operates close to Shannon capacity. The decoder at the destination utilizes source correlation as it knows that the data received via different routes is essentially the same.

RESCUE is a three-year FP7 project that officially started in November 2013. Work Package 2 (WP2) "code and algorithm design and optimization" started in the beginning of year 2014, and it will continue until the end of July 2016. In the beginning, the role of WP2 has been to identify, develop, and study channel coding and decoding methods as well as source-correlation estimation algorithms applicable to the RESCUE system. Recently, a new research item to study optimal transmit power allocation has started. While WP2 deals mainly with the physical layer functionality, WP1 addresses the more fundamental information theoretic and wireless access related aspects of cooperative multi-route relaying. On the other hand, WP3 takes the challenge of designing the necessary matching packet-based higher layer protocols such as multi-rate coding control, medium access control (MAC), automatic repeat request (ARQ) protocol, and routing. One essential task of WP2 is to support the development of the higher layer functionalities. To this end, in order to enable fast system level simulations, totally new methods of abstraction of the physical layer coding are under development in WP2. Finally, the work from WP2 and WP3 will be integrated together by WP4 to implement and demonstrate the operation of the system over-the-air on an software-defined-radio (SDR) testbed platform. Due to the common objectives, work is carried out in close cooperation between all the technical work packages.

This deliverable provides initial results and descriptions of the coding/decoding and source-correlation estimation algorithms considered in the RESCUE project. Chapter 2 addresses a simple network model consisting of a single source, a set of parallel relay nodes, and one destination node. Here, the state-of-the-art coding and decoding methods are motivated and reviewed, and some new performance results are shown. The iterative decoding at the destination can benefit from the knowledge of the bit error probabilities of each of the relayed information sequences. Thus, one of the needed algorithmic functionalities is correlation estimation that attempts to measure the bit error probabilities. In Chapter 3, advances in the correlation estimation are presented. In Chapter 4, more

general system models are considered. These include non-orthogonal channel access for the relay transmissions via interleave division multiple access (IDMA), multi-hop networks where the destination is more than two hops away from the source, and multiple-access relaying where two source nodes utilize a single relay node and communicate to a single destination node. Finally, Chapter 5 describes the new simulation abstraction concept, “black box”, that aims to enable system level development and simulations. Furthermore, some preliminary code design choices for the SDR implementation are disclosed.

2. Multi-route Relaying

This chapter addresses a simple multi-route relaying network model consisting of a single source, a set of parallel relay nodes, and one destination node as shown in Figure 2.1. Communication takes place in two phases. In phase one, the source transmits and the other nodes receive. In phase two, the relays transmit by using orthogonal radio resources, for example one at a time. There are one or more relays that take part in forwarding, and the direct link between the source and the destination may or may not exist. The principles of the coding and decoding algorithms based on distributed turbo codes, as first proposed in [ZHA+12; AM12a; ZCA+12], are described. Numerical results of the performance in terms of bit error rate (BER) and frame error rate (FER) are shown for some basic topologies, and compared to the performance figures predicted by the related theory.

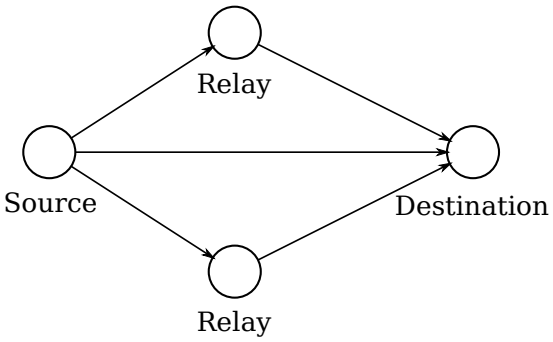

Figure 2.1: The general system model for multi-route relaying.

2.1 System Models and Theoretical Background

The research on cooperative communications using joint source, channel and network coding, has recently attracted a lot of attention with the recognition of significant importance. In cooperative communication systems, multiple mobile devices configure a virtual multi-terminal environment, and join in network-level cooperation, rather than assembling a set of point-to-point (P2P) connections. In this section, we consider the fundamentals of multi-route relaying problem from the viewpoint of network information theory.

2.1.1 Single-Relay Model

A single-relay model is a special case of the system shown in Figure 2.1, where just one relay node assists the destination to recover the source information. The single-relay model can be seen as an application of the theorem for *source coding with a helper* [GK11], in which the achievable compression rate region of correlated sources is characterized. An example of the achievable compression rate region is shown in Figure 2.2 (simplified from [ZCH+14]). The information sent from the source can be recovered by the destination only when the compressed rate pair falls into this area. For instance, consider the case that two binary information sequences $\mathbf{u}_1$ by the source and $\mathbf{u}_2$ by the relay are separately encoded, and jointly decoded at the destination. Here, $\mathbf{u}_1$ and $\mathbf{u}_2$ are compressed at the rates R_1 and R_2, respectively. When applying the compression theorem to the context of transmitting over wireless channels, R_1 and R_2 translate to the normalized channel capacities of the source-destination and relay-destination channels [ZCH+14]. The achievable rate region is given by

$$\begin{cases} R_1 & \geq & H(\mathbf{u}_1|\hat{\mathbf{u}}_2), \\ R_2 & \geq & I(\mathbf{u}_2;\hat{\mathbf{u}}_2), \end{cases} \tag{2.1}$$

where $\hat{\mathbf{u}}_2$ is the estimate of $\mathbf{u}_2$ at the destination, and $H(\cdot|\cdot)$ indicates conditional entropy and $I(\cdot;\cdot)$ mutual information. Here, $\hat{\mathbf{u}}_2$ serves as side information for the decoding of $\mathbf{u}_1$, which does not have to be perfect. With the help of $\hat{\mathbf{u}}_2$, R_1 can be further reduced to less than the entropy $H(\mathbf{u}_1)$. The correlation of the sources can be modeled by the bit flipping model as a result of channel decoding at the relay [LTA+11], i.e., $\mathbf{u}_2 = \mathbf{u}_1 \oplus \mathbf{e}$ and $\Pr(\mathbf{e}=1) = p_e$, where p_e is the bit-flipping probability (or BER) and $\oplus$ denotes binary exclusive OR operation. Assume that the appearance probabilities of the source bits 0 and 1 are equal. Then, $H(\mathbf{u}_1) = H(\mathbf{u}_2) = 1$, $H(\mathbf{u}_1|\mathbf{u}_2) = H_b(p_e)$, where $H_b(p_e) = -p_e \log_2(p_e) - (1-p_e)\log_2(1-p_e)$ is the binary entropy function.

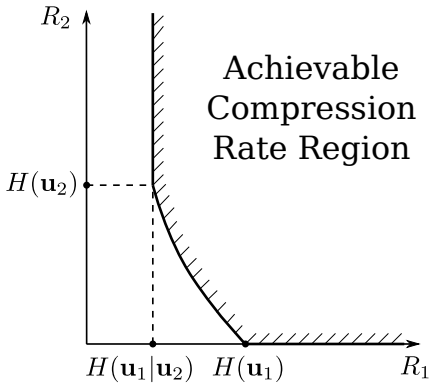

Figure 2.2: The achievable compression rate region of theorem for source coding with a helper.

Now consider a one-way relaying system, where the relay does not aim to perfectly recover the original information transmitted by the source, but it only "extracts" the source information, even though the relay knows that extracted sequence may contain some errors. This greatly reduces the computational complexity at the relay. The extracted sequence represents an estimate of the original information sequence, which is then interleaved and transmitted to the common destination. Obviously, the original and extracted sequences are correlated. As shown in [Tho08; AM12b; AM12a; CIA+12], even though extraction has relative weak error correction performance at the relay, excellent performance after joint decoding at the destination can still be achieved through the log-likelihood ratio (LLR) exchange between the decoders, where the correlation of the intra-link is taken into account.

Obviously, the performance can be further improved by performing FEC decoding at the relays as well. In this case though, the errors in the forwarded sequences become bursty instead of independent. Thus, it is imperative that the correlation is determined for each code block separately instead of employing average BER estimates.

2.1.2 CEO Relaying Model

In the single-relay model, there is only one relay, and the direct link between the source and the destination always exists. As an extension of single-relay model, a relay system with multiple relays and in the case when the direct link is non-existent (negligible), is also of interest to the RESCUE project. With the links-on-the-fly concept, all the messages forwarded by the relays are potentially lossy, and the destination intends to recover the original information transmitted from the source based on the multiple erroneous messages forwarded by the relays. It is clear that if all the forwarded sequences are erroneous, the destination cannot fully recover the original data either. Instead, some *distortion*, i.e., non-zero BER, will remain after the iterative joint decoding at the destination as well. This is called the error floor since it cannot be reduced by increasing the SNRs of the relay-to-destination links.

The problem of combining data from uncertain observers – relays in our case – is referred to as the the chief executive officer (CEO) problem [BZV96] in network information theory. Here, for simplicity, we assume the error probabilities happening in the source-relay links are fixed values, and the whole system is referred to as parallel CEO relaying. It should be emphasized here that the parallel CEO relaying model is equivalent to a wireless sensor network (WSN) model where the different sensors are observing the same source phenomenon, and the observation errors are modeled by bit-flipping. In [ZHA+12; HZA+13], we intensively studied the coding/decoding design for WSNs from the viewpoint of the CEO problem.

The quadratic Gaussian CEO problem in which the source and the multiple observations are assumed to be jointly Gaussian distributed, was studied in [Ooh98; VB97]. Besides the theoretical work, a successive coding and decoding algorithm was proposed in [BS05] based on the derived rate-distortion function for the parallel Gaussian CEO problem, and the optimal rate allocation scheme in order to achieve the minimal distortion under a sum-rate constraint was further considered in [BS09] for the successive coding/decoding strategy. An iterative joint decoding algorithm for the binary data gathering WSNs was proposed in [HBP08], where the convolutional code is applied as the coding scheme at the sensor node to protect the data transmitted over noisy links between the sensors and the fusion center (FC). In [RYA11], a coding scheme based on the parallel concatenated convolutional codes (PCCC) was proposed. They used a joint decoding algorithm, which utilizes the correlation knowledge among

the observations of the sensors by weighting the extrinsic log-likelihood ratios (LLRs) by the error probabilities of erroneous observations. Moreover, the capacity of the parallel channel was derived for verifying the bit error rate (BER) performance by taking into account the error probability of the observed data sequence. In [RA12], an adaptive bi-modal decoder for a binary source estimation involving two sensors was proposed based on the modified extrinsic information transfer (EXIT) chart analysis.

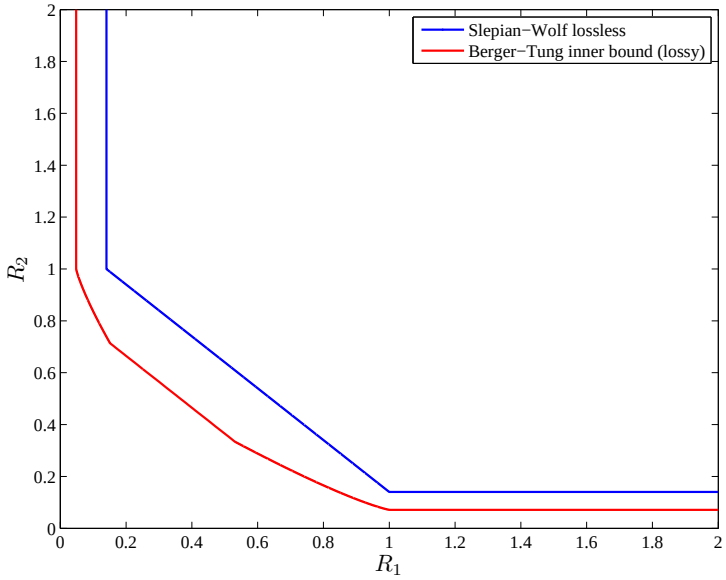

Figure 2.3: The admissible rate region of Slepian-Wolf theorem and rate-distortion region of Berger-Tung inner bound.

Let us take the CEO relaying model with two relays as an example, and let $\mathbf{u}_1$ and $\mathbf{u}_2$ denote the data sequences forwarded by the two relays, respectively. Here, the destination aims to resolve both two relayed sequences. Assume $\mathbf{u}_1$ and $\mathbf{u}_2$ are described at rates R_1 and R_2, respectively, then the rate-distortion derived based on the Berger-Tung inner bound [GK11] is

$$\begin{cases} R_1 & \geq & I(\mathbf{u}_1;\mathbf{v}_1|\mathbf{v}_2), \\ R_2 & \geq & I(\mathbf{u}_2;\mathbf{v}_2|\mathbf{v}_1), \\ R_1+R_2 & \geq & I(\mathbf{u}_1,\mathbf{u}_2;\mathbf{v}_1,\mathbf{v}_2), \end{cases} \tag{2.2}$$

where $\mathbf{v}_1$ and $\mathbf{v}_2$ are the descriptions of $\mathbf{u}_1$ and $\mathbf{u}_2$, respectively, created and forwarded by the relays. The admissible rate-distortion region is depicted in Figure 2.3 with some given distortion levels. As a special case, if the distortions for $\mathbf{u}_1$ and $\mathbf{u}_2$ are both 0, the problem has already been solved by the Slepian-Wolf theorem [SW73], with which the admissible rate region is

$$\begin{cases} R_1 & \geq & H(\mathbf{u}_1|\mathbf{u}_2), \\ R_2 & \geq & H(\mathbf{u}_2|\mathbf{u}_1), \\ R_1+R_2 & \geq & H(\mathbf{u}_1,\mathbf{u}_2). \end{cases} \tag{2.3}$$

The admissible rate region of the Slepian-Wolf theorem is also shown in the same figure for comparison. It is clearly found that by accepting some distortion in $\mathbf{u}_1$ and $\mathbf{u}_2$ at the destination, the rate-distortion region of CEO relaying model can be further expanded. This indicates that further compression at the relays is allowed, or equivalently, in the wireless channel transmission, transmit powers can be reduced.

2.2 Distributed Turbo Codes – Coding and Decoding

2.2.1 Single-Relay Model

In our simple one way relay system, both the relay and the destination receive the signal from the source node during phase 1. At the relay node, the information (systematic) bits are recovered, either by performing channel decoding or even by extracting the systematic part of the coded bits, before being re-transmitted. During phase 2,

the recovered bits (may contain some errors) are interleaved, re-encoded again, and forwarded to the destination node.

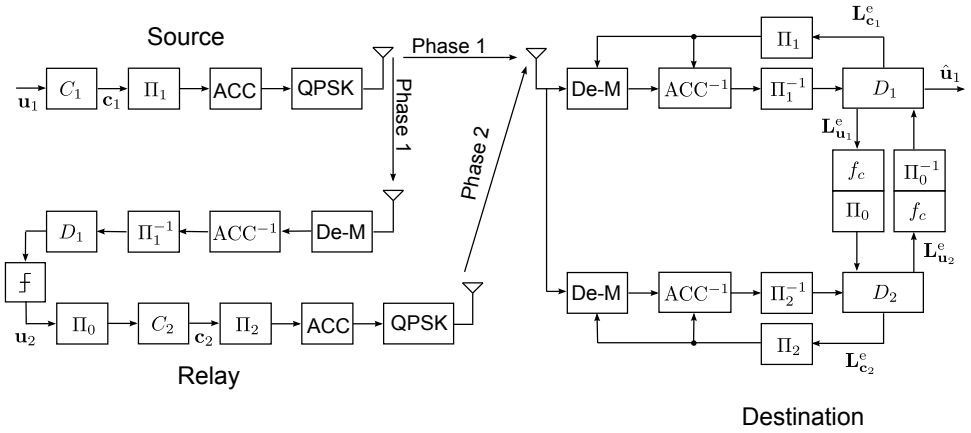

Figure 2.4: The structure of the relay system.

The block diagram of the proposed relay system is shown in Figure 2.4. In this system, we do not need strong codes: only memory-1 half rate ($R = 1/2$) systematic non-recursive convolutional code (SNRCC) is adopted for both encoders C_1 and C_2. At the source node, the original information bits b_1 are first encoded by C_1. After that, the encoded bit sequences are interleaved by Π_1 and doped-accumulated by ACC (with a doping rate $P_{d1} \geq 1$). Then, they are modulated into symbols s by using quadrature phase-shift keying (QPSK) modulation, and transmitted to both the relay and the destination during the first time slot. The details of the doped accumulator are shown in Figure 2.5.

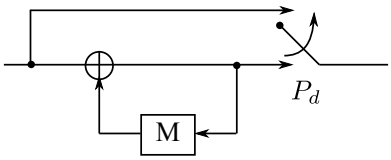

Figure 2.5: Doped accumulator. The switch selects every P_dth output bit from the accumulator, while the other $P_d - 1$ outputs are systematic.

At the relay node, the received signals first go through the demapper, ACC^{-1} and the de-interleaver Π_1^{-1}. Then, the original information bits $\mathbf{u}_1$ are recovered by making hard decisions of the output of the decoder D_1, which is denoted as $\mathbf{u}_2$. After that, the recovered bits are interleaved by Π_0 and then go through the channel encoder C_2, the interleaver Π_2 and the ACC (with doping rate P_{d2}). Then the data are modulated into s_r, and transmitted to the destination during the second time slot.

At the destination node, the received signals y_{sd} and y_{rd} first go through the horizontal decoding processes as can be seen in Figure 2.4, where the combination of the demapper and the ACC exchange information with the channel decoders through horizontal iterations (HI) [AM12a]. After every HI, the extrinsic LLRs obtained from the two decoders D_1 and D_2 are also exchanged with several vertical iterations (VI), through an LLR updating function f_c [GZ05]. The f_c function is defined as

$$f_c(\mathbf{L}, p_e) = \ln \frac{(1-p_e)\exp(\mathbf{L}) + p_e}{(1-p_e) + p_e \exp(\mathbf{L})}, \tag{2.4}$$

where $\mathbf{L}$ represents the input LLR sequence into the f_c function, which are $\mathbf{L}^{\mathrm{e}}_{\mathbf{u}_1}$ and $\mathbf{L}^{\mathrm{e}}_{\mathbf{u}_2}$ as shown in Figure 2.4. Function f_c can be obtained by first converting the LLR into the probabilities of the systematic bits being "0" and "1", and then modifying the values by taking into account the knowledge of p_e. The purpose of function f_c is to avoid the error propagation while exchanging likelihood information between HI and VI. By doing this, the extrinsic LLR (systematic part) forwarded from the relay helps decoding of the original bits by exploiting the correlation knowledge between the source and the relay. Finally, the original information can be recovered by making hard decisions of the a posteriori LLRs at the output of D_1.

2.2.2 CEO Relaying Model

2.2.2.1 Transmitter

Figure 2.6 illustrates the CEO relaying model to be analyzed. An uncoded binary source $\mathbf{u}$, where the bits are independent and evenly distributed between zeros and ones, is transmitted to multiple relays. Since hard decisions are always performed at the relays, we may simply use a bit-flipping model to randomly generate errors in the data sequence. The received information $\mathbf{u}_k$ can be seen as the output of a binary symmetric channel (BSC) with associated crossover probability p_k when $\mathbf{u}$ is the input, i.e., $\mathbf{u}_k = \mathbf{u} \oplus \mathbf{e}_k$ where "$\oplus$" denotes the binary exclusive OR operation. Consequently, the bit sequences are correlated with each other since they have the common input $\mathbf{u}$ of the independent BSCs.

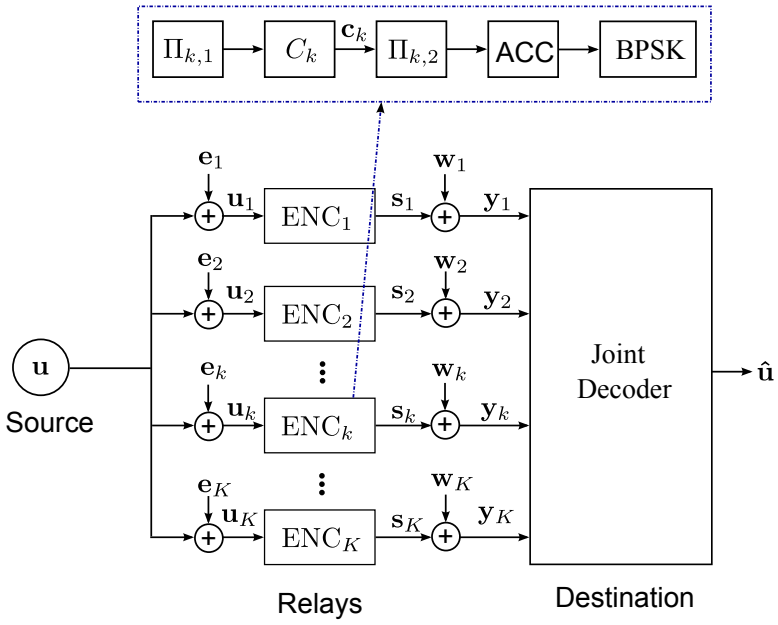

Figure 2.6: A schematic diagram of a parallel CEO relaying model [HZJ+14].

The k-th relay encodes its data $\mathbf{u}_k$ by an encoder ENC_k and transmits the corresponding coded data to the destination. For simplicity, we assume simple serially concatenated convolutional codes with binary data transmission. The data $\mathbf{u}_k$ is, first of all, interleaved by an interleaver $\Pi_{k,1}$ whose role is to enable the global iterative decoding process to utilize the correlation knowledge. The interleaved sequence is then encoded by an encoder C_k resulting in the coded sequence $\mathbf{c}_k$. It is further interleaved by another interleaver $\Pi_{k,2}$, the length of which depends on the code rate R_k^{c} of the encoder C_k. After that, the interleaved version of $\mathbf{c}_k$ is doped-and-accumulated by a so-called accumulator ACC [AM12a] with a doping ratio P_d. Finally, the modulated symbol sequence $\mathbf{s}_k \in \{+1,-1\}$, generated by binary phase-shift keying (BPSK) modulation for the doped-accumulated binary sequence, is transmitted over AWGN channels to the destination at different time slots. Therefore, the received signal $\mathbf{y}_k$ at the destination from the k-th relay is simply expressed as

$$\mathbf{y}_k = \mathbf{s}_k + \mathbf{w}_k, \tag{2.5}$$

where $\mathbf{w}_k \sim \mathscr{CN}(0,\sigma^2)$ is a complex white Gaussian noise sequence with the variance per dimension σ^2.

2.2.2.2 Receiver

The block diagram of the joint decoding technique is shown in Figure 2.7. Because of the fact that the received data sequences from the relays are highly correlated, *global iteration* (GI) is introduced in the iterative decoding process with the view to utilizing the correlation knowledge, i.e., the extrinsic LLR is exchanged between GI and local iteration (LI) to enhance the BER performance.

The decoding process is divided into following steps:

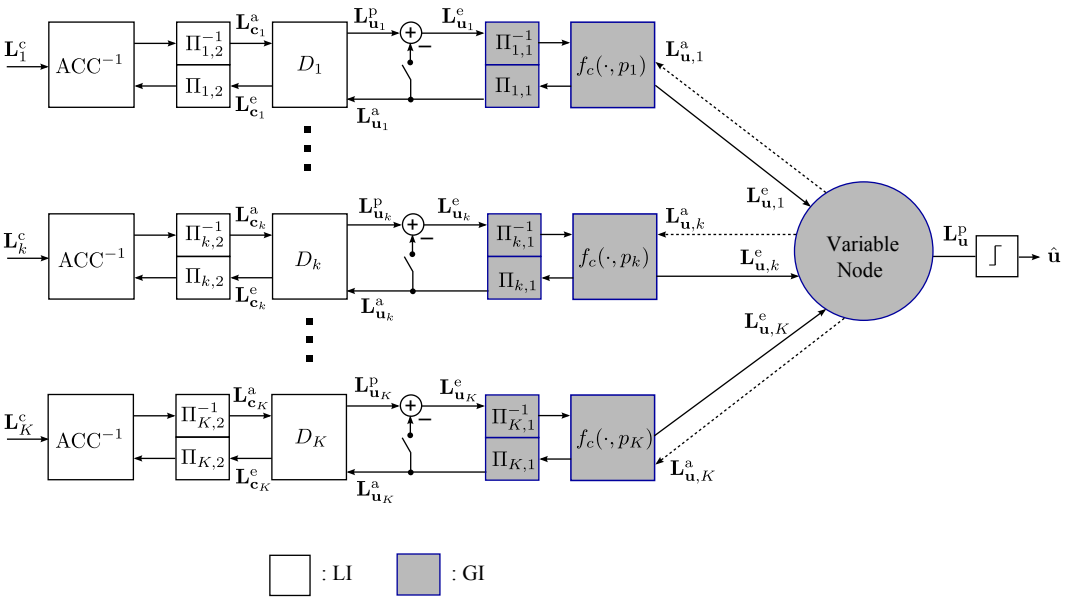

Figure 2.7: The joint decoding strategy utilizes correlation knowledge among the relays' data through global iteration [HZJ+14].

1. Initialization: The channel state information is fully known to the destination. Thereby, after receiving the signal $\mathbf{y}_k$ from the k-th relay, the channel LLR $\mathbf{L}_k^{\mathrm{c}}$ is calculated by

$$\mathbf{L}_k^{\mathrm{c}} = \frac{2}{\sigma^2}\Re(\mathbf{y}_k), \tag{2.6}$$

   where $\Re(\cdot)$ takes the real part of a complex value in its argument. In addition, the extrinsic LLR $\mathbf{L}_{\mathbf{c}_k}^{\mathrm{e}}$ of the coded bits and the *a priori* LLR $\mathbf{L}_{\mathbf{u}_k}^{\mathrm{a}}$ of the systematic bits, which are corresponding to the *a priori* LLR fed back to ACC^{-1} after interleaving, and the *a priori* LLR to D_k, respectively, are set to 0.

2. LIs are performed between ACC^{-1} and D_k, $k = 1, \cdots, K$, simultaneously.

3. The extrinsic LLR $\mathbf{L}_{\mathbf{u}_k}^{\mathrm{e}}$, which is obtained by subtracting the *a priori* LLR $\mathbf{L}_{\mathbf{u}_k}^{\mathrm{a}}$ from the *a posteriori* LLR $\mathbf{L}_{\mathbf{u}_k}^{\mathrm{p}}$, is deinterleaved by $\Pi_{k,1}^{-1}$ and then updated through function f_c as

$$\mathbf{L}_{\mathbf{u},k}^{\mathrm{e}} = f_c\{\Pi_{k,1}^{-1}(\mathbf{L}_{\mathbf{u}_k}^{\mathrm{e}}), p_k\}. \tag{2.7}$$

4. A degree K variable node combines $K-1$ extrinsic LLRs $\mathbf{L}_{\mathbf{u},j}^{\mathrm{e}}$, $j \neq k$, obtained as the results of LIs, to calculate the message fed back to the decoder D_k of the k-th LI. Thus, the *a priori* LLR $\mathbf{L}_{\mathbf{u},k}^{\mathrm{a}}$ is then obtained as

$$\mathbf{L}_{\mathbf{u},k}^{\mathrm{a}} = \sum_{j \in \kappa \backslash k} \mathbf{L}_{\mathbf{u},j}^{\mathrm{e}}, \tag{2.8}$$

   where $\kappa = \{1, 2, \cdots, K\}$ is the set of the indices of the relays, and $\kappa \backslash k$ means removing k from the set κ.

5. The output of $f_c(\mathbf{L}_{\mathbf{u},k}^{\mathrm{a}}, p_k)$ is interleaved by $\Pi_{k,1}$ to form the *a priori* LLR $\mathbf{L}_{\mathbf{u}_k}^{\mathrm{a}}$ which is fed back to D_k in the corresponding k-th LI.

The decoding process is performed in an iterative manner where Steps 2) to 5) are repeated with the switches shown in Figure 2.7 being closed except in the final iteration, since the exchanged information between decoders should be extrinsic according to the turbo principle.

In the final iteration, the switches are all opened, and a hard decision on $\mathbf{u}$ is made to make a final estimate $\hat{\mathbf{u}}$ of $\mathbf{u}$, based on the *a posteriori* LLR $\mathbf{L}_{\mathbf{u}}^{\mathrm{p}}$ originated by summing up all the deinterleaved and f_c-updated versions of the *a posteriori* LLR $\mathbf{L}_{\mathbf{u}_k}^{\mathrm{p}}$.

2.3 Numerical Results

2.3.1 Single-Relay Model

Three relay location scenarios are considered, as shown in Figure 2.8. Generally, the relay node can be allocated closer to the source node in Location A or closer to the destination in Location B, or the three components keep the same distance from each other in Location C. The geometric gain of the source-relay (sr) link with regard to the source-destination (sd) link can be defined as

$$G_{sr} = \left(\frac{d_{sd}}{d_{sr}}\right)^{\alpha}, \tag{2.9}$$

where the path loss exponent α is assumed to be 3.52 [YG11] in our simulations. It is straightforward to derive the geometric-gain of the relay-destination (rd) link G_{rd} in the same way. Moreover, without losing the generality, the geometric-gain of the source-destination link, G_{sd}, is fixed to one. Therefore the received signals y_{ij} ($ij \in \{sr, sd, rd\}$) at the relay and the destination node can be expressed as:

$$y_{sr} = \sqrt{G_{sr}} \cdot h_{sr} \cdot s + n_{sr}, \tag{2.10}$$

$$y_{sd} = \sqrt{G_{sd}} \cdot h_{sd} \cdot s + n_{sd}, \tag{2.11}$$

$$y_{rd} = \sqrt{G_{rd}} \cdot h_{rd} \cdot s_r + n_{rd}, \tag{2.12}$$

where s and s_r represent the symbols transmitted from the source and the relay, respectively. The fading channel gain, h_{ij}, is equal to one in the additive white Gaussian noise (AWGN) channel. The notation n_{ij} represents the zero-mean AWGN noise of the three links with variance σ_{ij}^2. The signal-to-noise ratio (SNR) of source-relay and relay-destination links at each location scenario are evaluated as follows: given the path loss parameter α equals to 3.52 [YG11], we have SNR_{sr} = SNR_{sd} + 21.19 dB and SNR_{rd} = SNR_{sd} + 4.4 dB in Location A; SNR_{sr} = SNR_{sd} + 4.4 dB and SNR_{rd} = SNR_{sd} + 21.19 dB in Location B; SNR_{sd} = SNR_{rd} = SNR_{sr} in Location C.

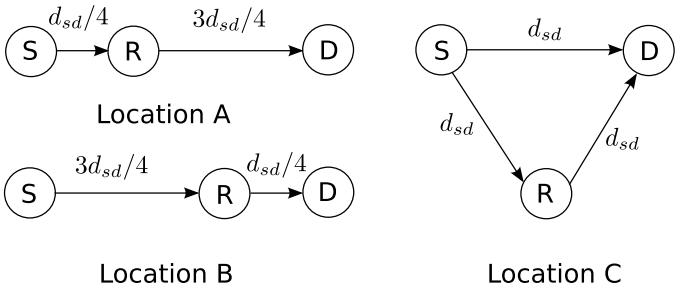

Figure 2.8: Simulation setups for single-relay transmission. d_{sd} denotes the distance of the source-relay link [CZA+12].

Figure 2.9 shows the BER performances of the proposed relay system using QPSK with natural (Gray) mapping rule, where the frame length of the transmitted information is set at 10000 bits in the simulations. Based on the EXIT analysis, 30 horizontal iterations are performed at the destination node and meanwhile 5 vertical iterations take place between the two decoders D_1 and D_2 during each horizontal iteration.

The turbo cliff can be achieved by using our technique in the relay system over AWGN channels. It can be seen from Figure 2.9 that, when performing the channel decoding at the relay node, the BER performance in Location A is much better than that of the other cases. The reason is that, when the relay is close to the source, the geometric gain of the intra-link is large and the intra-link error probability p_e is very small. In other words, the recovered bits at the relay node are highly correlated with the original information at the source node, and the decoder D_2 at the destination is able to provide very reliable extrinsic LLRs of the information bits, which can be fed into the decoder D_1 as the a priori information. Hence, the Location C's case has the worst BER performance because there is no geometric gain when the source, relay and destination nodes are equally separated.

On the other hand, Figure 2.9 also presents the BER curves by using extract-and-forward (EF) relay strategy, where only the systematic part of the coded bits are extracted, without performing channel decoding at relays. It can be clearly seen that the intra-link BER performance of the EF scheme is worse than that of the decode-and-forward

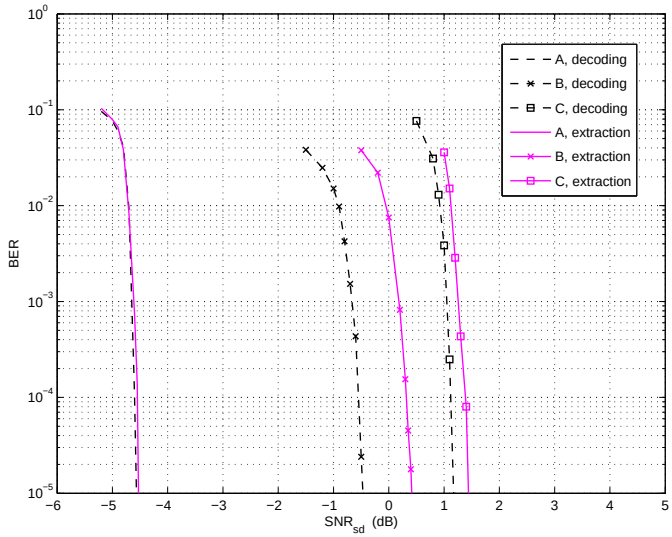

Figure 2.9: BER performance of the proposed system with QPSK in AWGN channel [CZA+12].

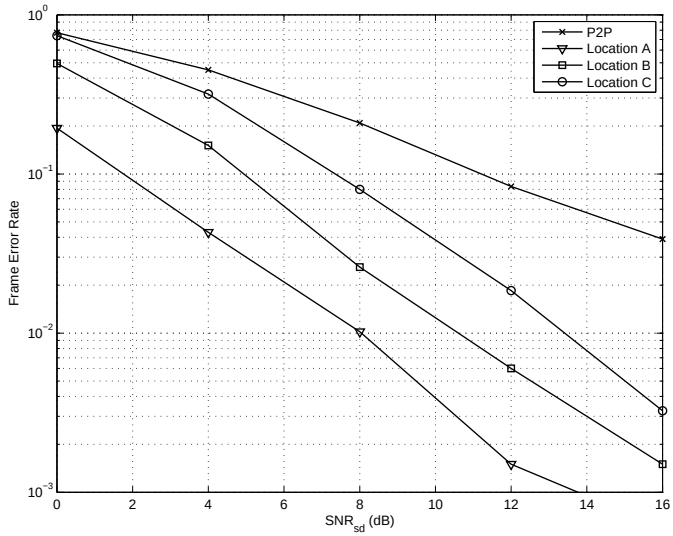

Figure 2.10: FER performance of the proposed system with QPSK in block Rayleigh fading channel [CZA+12].

(DF) scheme. However, it has to be noted that the EF scheme can achieve almost the same BER performance as DF in Location A. This is because that the intra-link is very strong when the relay is close to the source node, and both of the DF and EF strategies can almost fully recover the original bits at the relay. When the relay node is close to the destination as in Location B, there is about 1 dB gap between the BER curves of DF and EF schemes. In the case of Location C, the BER gap between DF and EF is much smaller than that of Location B's case.

According to [CBV05], with code rate 1/2, the Shannon/SW limit for Location C for Gaussian codebook is -1.55 dB. Therefore, as can be seen from Figure 2.9, the gap of the proposed system to the theoretical limit in Location C is 2.75 dB.

Finally, the frame-error-rate (FER) performance in block Rayleigh fading channels is shown in Figure 2.10. The interleaver lengths are set at 4400 bits. The point-to-point (P2P) transmissions are simulated for comparison. Similarly to the AWGN channel cases, the proposed system achieves better FER performance when the relay is closer to the source.

2.3.2 CEO Relaying Model

A series of simulations has been conducted to verify the results of our proposed coding/decoding techniques. This subsection provides the results of the simulations. The common parameters assumed in the simulations were set as follows

- Block length $n = 10000$ bits.
- Interleavers: random.
- Encoder C_k, $k = 1, \cdots, K$: rate $R_k^c = \frac{1}{2}$ nonrecursive systematic convolutional code with generator polynomial $G = [03, 02]_8$, where $[\cdot]_8$ represents the argument is an octal number.
- Doping ratio $P_d = 1$.
- Decoding algorithm for D_k and ACC^{-1}: log-maximum *a posteriori* (MAP).
- The number of iterations: 50 times.
- The SNR of each relay node is assumed to be the same.

Figure 2.11 illustrates the BER performance of the technique presented in [ZHA+12] and [HZA+13] with the number of relays $K = \{2,4,6,8\}$. The new results of the theoretical analysis presented in [HZJ+14] are also shown. In the simulations, the error probabilities p_k were all set to 0.01. It can be clearly seen that in all the cases, the BER curves exhibit sharp drop in the values at their corresponding threshold SNR values, like turbo-cliff of the turbo-codes. The difference between the threshold SNR obtained by the simulations and the theoretical analysis are $\{1.61, 1.65, 1.88, 1.92\}$ dB for $K = \{2,4,6,8\}$. Furthermore, the sharp decrease in BER suddenly plateaus at higher SNR values, where the error floor appears.

Figure 2.12 shows the BER performance with $K = \{3,5,7\}$, where the error probabilities p_k were set at uneven values that are shown in the caption of Figure 2.12. Even in these cases, the BER performance gap to the theoretical limits are about $\{1.52, 1.73, 1.8\}$ dB.

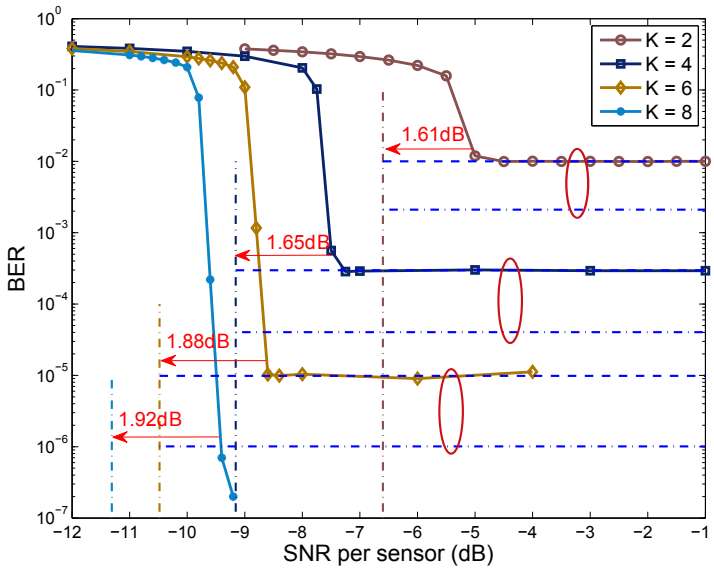

Figure 2.11: BER performance of our proposed technique with the number of relays $K = \{2,4,6,8\}$. p_k are set at 0.01. The corresponding SNR_{lim} are plotted in vertical dash-dot lines. The approximated error floors and the lower bounds p_{lb} of the error floors are presented in horizontal dashed and dash-dot lines, respectively [HZJ+14].

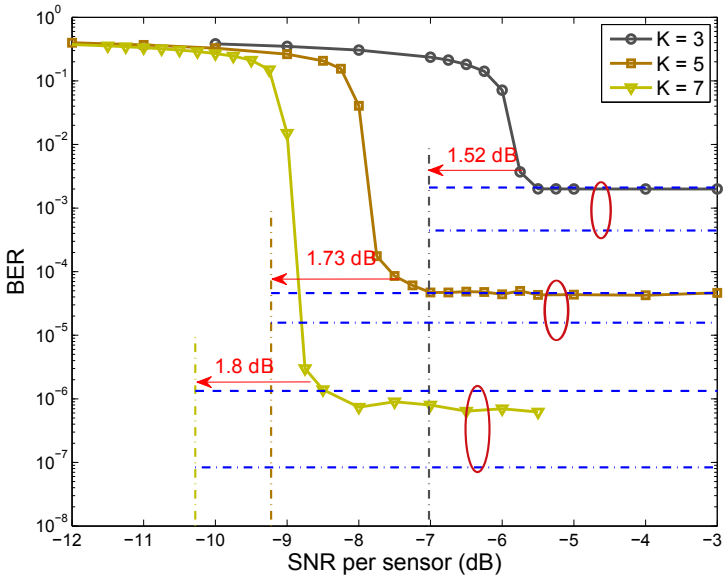

Figure 2.12: BER performance comparison with the number of relays $K = \{3,5,7\}$. The observation error probabilities are distributed as $p_k = \{0.025, 0.075, 0.002\}$, $p_k = \{0.0145, 0.005, 0.025, 0.015, 0.03\}$ and $p_k = \{0.01, 0.015, 0.02, 0.05, 0.005, 0.0003, 0.02\}$ [HZJ+14].

It is also found that the error floors shown in Figures 2.11 and 2.12 are placed between the results of the Poisson-binomial approximation (upper bound) and the rate-distortion lower bound. It is clearly seen that the error floors found by simulations match well with the values obtained in Poisson-binomial approximation. The elimination of the error floor is impossible since the errors are inserted before encoding at each relay node, even though the floor can be made very small because of the combined use of LI and GI.

3. Source Correlation Estimation

3.1 Source Correlation Estimation at the Destination

In order to utilize the correlation knowledge in the decoding process, the correlations need to be estimated somehow. The estimation may be carried out at the destination as part of the iterative decoding process so that after each global iteration the estimates are refined. In this section, several methods are described that can improve the estimation performance of the relay errors. With an improved estimation, the decoding performance of the destination can be significantly improved. Initially, the state of the art algorithm is repeated and its performance is presented. Then, the influence of the threshold T is investigated and an adjusted value is proposed. Moreover, the influence of the estimation variance on the decoding performance is described and methods for reducing the estimation variance, further improving the decoding performance. In addition to modifications of the state-of-the-art (SoTA) estimator, new estimators are presented. Finally, the performance of the proposed estimators is analyzed with the help of simulations.

3.1.1 State-of-The-Art Algorithm and Performance

In [HZA+13], we proposed a nonnegative constrained iterative algorithm to estimate the observation error probabilities, which is also referred as the source correlation. Assuming that the bit decision errors made by the relays are uncorrelated, and that the bit error probability at relay i is p_i, the following pairwise equations hold

$$q_{ij} = p_i(1-p_j) + p_j(1-p_i), \tag{3.1}$$

for $i = 1,\cdots,K$; $j = 1,\cdots,K$; and $i \neq j$. Here, q_{ij} is the pairwise bit error probability, i.e., the probability that a bit in the sequence of relay i differs from the corresponding bit in the sequence of relay j. We choose K pairs of the correlation equations in [HZA+13] to estimate the error probabilities p_i as

$$\begin{aligned} &\hat{p}_i + \hat{p}_j - 2\cdot\hat{p}_i\cdot\hat{p}_j = \hat{q}_{ij}, \\ \text{where, } &i = 1\cdots K, \\ &j = i+1 \text{ if } i = 1\cdots K-1, \\ &j = 1 \text{ if } i = K, \end{aligned} \tag{3.2}$$

where following [GZ05], the *a posteriori* LLRs at the output of the two decoders are utilized in the pairwise error probability estimation as

$$\hat{q}_{ij} = \frac{1}{N}\sum_{n=1}^{N} \frac{\exp(L^{\mathrm{p}}_{\mathbf{u}_i,n}) + \exp(L^{\mathrm{p}}_{\mathbf{u}_j,n})}{[1+\exp(L^{\mathrm{p}}_{\mathbf{u}_i,n})]\cdot[1+\exp(L^{\mathrm{p}}_{\mathbf{u}_j,n})]}, \tag{3.3}$$

where N represents the number LLR pairs with their absolute values larger than a given threshold T. Since the reliability of $\hat{q}_{ij}$ is influenced by N, it is important to choose an appropriate T value. However, how to determine the optimal T was not studied in [HZA+13].

We can reformulate (3.2) by introducing the identity matrix $\mathbf{I}$ of size K and a matrix $\mathbf{J}$ defined by (3.5), into the following form:

$$[(\mathbf{I}+\mathbf{J}) - 2\cdot\mathrm{diag}(\hat{\mathbf{p}})\cdot\mathbf{J}]\cdot\hat{\mathbf{p}} = \hat{\mathbf{q}}, \tag{3.4}$$

where, $\hat{\mathbf{p}} = [\hat{p}_1, \hat{p}_2, \cdots, \hat{p}_K]^T$, and $\hat{\mathbf{q}} = [\hat{q}_{12}, \hat{q}_{23}, \cdots, \hat{q}_{K1}]^T$. The $\mathrm{diag}(\cdot)$ is the operator that forms a diagonal matrix from its argument vector, and $\mathbf{J}$ is defined as follows:

$$\mathbf{J} = \begin{bmatrix} 0 & 1 & 0 & 0 & \cdots 0 \\ 0 & 0 & 1 & 0 & \cdots 0 \\ \vdots & \vdots & \vdots & \vdots & \vdots \\ 1 & 0 & 0 & 0 & \cdots 0 \end{bmatrix}. \tag{3.5}$$

Now, our objective is to find a nonnegative vector $\hat{\mathbf{p}}$ that minimizes $\|\mathbf{A}\hat{\mathbf{p}} - \hat{\mathbf{q}}\|^2$, which is formulated as follows:

$$\begin{aligned} &\min \ \|\mathbf{A}\hat{\mathbf{p}} - \hat{\mathbf{q}}\|^2 \\ &\text{s.t } \hat{\mathbf{p}} \succeq \mathbf{0}, \end{aligned} \tag{3.6}$$

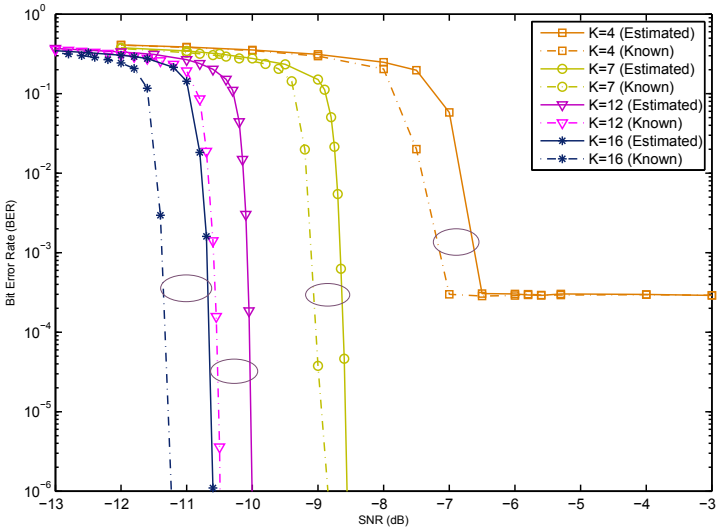

Figure 3.1: BER performance comparison for different numbers of relays [HZA+13].

where, $\mathbf{A} = [(\mathbf{I}+\mathbf{J}) - 2 \cdot \mathrm{diag}(\hat{\mathbf{p}}) \cdot \mathbf{J}]$. Now, vector $\hat{\mathbf{p}}$ is also inside matrix $\mathbf{A}$. Therefore, problem (3.6) is solved multiple times, and matrix $\mathbf{A}$ is updated in every iteration. The iterative algorithm is summarized in Algorithm 1. In this algorithm, we use the standard nonnegative least squares (*lsqnonneg*) [CP07] proposed by Lawson and Hanson.

Algorithm 1: p estimator

Input: $\hat{\mathbf{q}}$, ε, Pre-defined maximum iterations IT_m
Output: $\hat{\mathbf{p}} \succeq \mathbf{0}$ such that $\hat{\mathbf{p}}$=arg min $\|\mathbf{A}\hat{\mathbf{p}} - \hat{\mathbf{q}}\|^2$
Initialization: $\hat{\mathbf{p}}^{(0)} = \mathbf{0}$, Calculate $\mathbf{A}$ and $\Delta(0) = \|\mathbf{A}\hat{\mathbf{p}}^{(0)} - \hat{\mathbf{q}}\|^2$
for $h = 1$ **to** IT_m **do**
  Calculate $\hat{\mathbf{p}}^{(h)}$ by solving (3.6) using *lsqnonneg* algorithm;
  Update $\mathbf{A} = [(\mathbf{I}+\mathbf{J}) - 2 \cdot \mathrm{diag}(\hat{\mathbf{p}}^{(\mathbf{h})}) \cdot \mathbf{J}]$;
  $\Delta(h) = \|\mathbf{A}\hat{\mathbf{p}}^{(h)} - \hat{\mathbf{q}}\|^2$;
  if $\Delta(h) \geq \Delta(h-1)$ **then**
    Stop;
  end
  if $\|\hat{\mathbf{p}}^{(h)} - \hat{\mathbf{p}}^{(h-1)}\|^2 \leq \varepsilon$ **then**
    $\hat{\mathbf{p}} = \hat{\mathbf{p}}^{(h)}$;
    Stop;
  end
end
$\hat{\mathbf{p}} = \hat{\mathbf{p}}^{(IT_m)}$;

Figure 3.1 shows the BER performances in AWGN channel for the cases where estimated $\hat{\mathbf{p}}$ and known $\mathbf{p}$ are used at the destination, with the number K of relays as a parameter. The decoding errors at relays were generated via the bit-flipping model with $p_i = 0.01$ for all i. At each relay, a half rate memory-1 nonrecursive systematic convolutional code and a doped accumulator with doping ratio 1 was used. In the error probability estimator, T and ε were set to 2 and 10^{-6}, respectively, and the maximum iteration times, IT_m, were set at 20.

It is found from the figure that the BER performance can be improved by increasing the number of relays K. With $K = 4$, the error floor can not be reduced to less than 10^{-4} by increasing per-link SNR, however it can be reduced to less than 10^{-6} with $K \geq 7$. Nevertheless, we believe that it is impossible to totally eliminate the error floor, even though it may happen at a very small BER region. The reason is because we can not completely eliminate the distortion due to the observation error, which is common to the CEO problems. Compared with the case where $\mathbf{p}$ is known, only $0.3 - 0.5$ dB loss in per-link SNR is observed when using estimated $\hat{\mathbf{p}}$, and the loss depends on the number K of the relays.

3.1.2 Modification of the SoTA Estimation Algorithms

3.1.2.1 Threshold Adaptation

According to (3.3), the pairwise error probability is estimated based on a subset of the received samples, which are selected based on the magnitude of their decoded LLR, where the threshold is given by T. The threshold has a significant influence on the position of the waterfall region. The optimal estimation threshold can be found by computing a look-up table for optimal thresholds for each link's SNR by simulating the decoding process with random data in an AWGN channel. Hence, the look-up table is pre-defined by simulations. The according algorithm is provided in Algorithm 2.

Algorithm 2: Computation of look-up table for optimal threshold

Input: ε, maximum iteration M, SNR list
Output: Look-up table $T(\mathrm{SNR})$
Initialization: $T(SNR) = 2.5$
for *n = 1* **to** *length(SNR)* **do**
  $t^{n,m} = T(SNR[n-1])$
  for $m = 1$ **to** M **do**
    Run Joint Decoder simulation with $SNR(n)$ and $T = t^{n,m}$, Output $\hat{\mathbf{p}}^{(n,m)}$
    if $MSE(\hat{\mathbf{p}}^{(n,m)}) \leq \varepsilon$ **then**
      $T(SNR(n)) = t^{n,m}$
      Exit **for**
    end
    if $MSE(\hat{\mathbf{p}}^{(n,m)}) \geq MSE(\hat{\mathbf{p}}^{(n,m-1)})$ **then**
      $T(SNR(n)) = t^{n,m-1}$
      Exit **for**
    end
    $t^{n,m+1} = t^{n,m} - 0.05$
  end
end

Basically, for each SNR the optimal threshold is determined as the T which minimizes the mean squared error between estimated and correct bit flipping probability p_k. It is assumed that the optimal T decreseases with increasing SNR, since decoding performance in the horizontal iterations in the destination is more reliable on its own and hence the LLR after horizontal iterations can also be considered more reliable at smaller values.

3.1.2.2 Reducing Estimation Variance

In the SoTA estimation algorithm, the error probability of the relays is calculated based on the estimated pairwise error probability between the relays. Though this estimator tends to be unbiased (see Section 3.1.4.1) at higher SNR, the variance of the estimated errors is also an important aspect, since it determines the accuracy of every single run of the estimator.

In particular, if the actual relay error is very low, it may happen during global decoding iterations that the reference estimator calculates an error probability close to zero. In this case, the update function f_c does not damp the relay's LLR and hence other relays are outvoted by this particular relay. Accordingly, the BER at the destination is determined by the error of this particular relay. The behaviour of this singular estimation is illustrated in Figure 3.2. Hence, it is not only necessary to have an unbiased estimation but also an accurate estimation with low variance. In the following, two approaches for reducing the estimation variance are described.

Estimation with Different Relay Combinations Let $\hat{\mathbf{p}} = E_T(q(\mathbf{K}))$ be the execution of the estimation via Algorithm 1 with the resulting estimated relay errors $\hat{\mathbf{p}}$ and the threshold T. There,

$$q(\mathbf{K}) = \{q_{\mathbf{K}_K,\mathbf{K}_1}\} \cup \{q_{\mathbf{K}_j,\mathbf{K}_{j+1}} | j \in \{1,2,\ldots,K\}\} \tag{3.7}$$

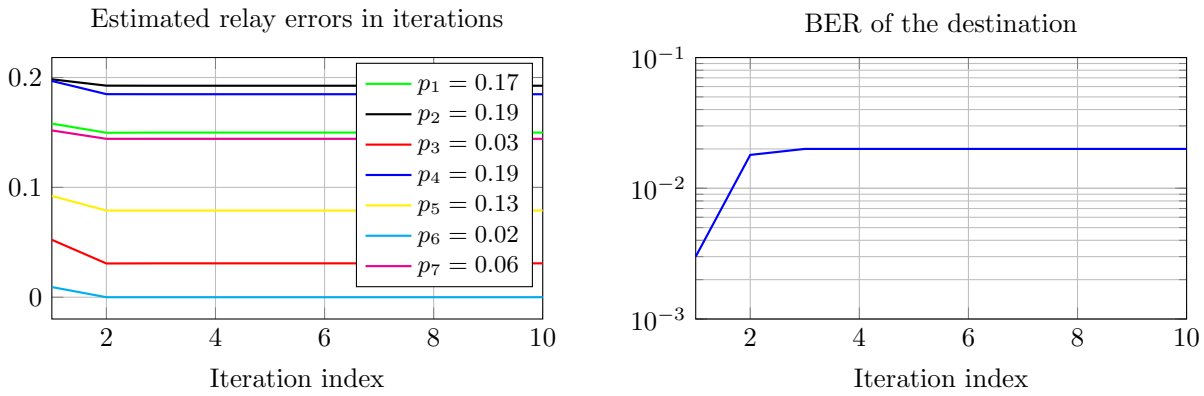

Figure 3.2: Example of singular estimation for $\hat{p}_6 \to 0$ and resulting BER. $K = 7$ with correct error probabilities in the legend and estimated values in the diagram. As the $\hat{p}_6 \to 0$, the BER at the destination tends to the BER of this particular relay.

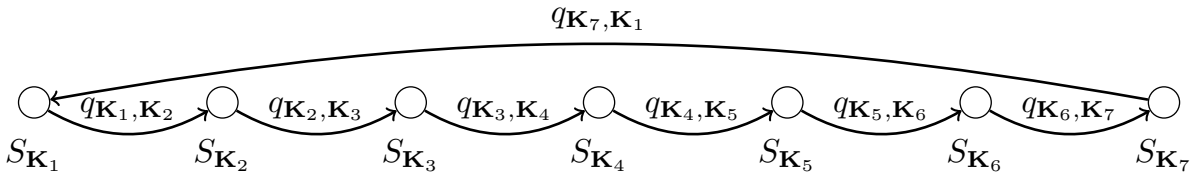

Figure 3.3: Illustration of selection of pairwise error probabilities.

describes the pairwise error probabilities between the relay pairs indexed in the vector $\mathbf{K}$, where $\mathbf{K}_j$ denotes the jth element of $\mathbf{K}$. The process of selecting the q_{ij} is illustrated in Figure 3.3 where S_u denotes LLR of the uth relay. The estimation of the relay errors of the proposed algorithm in [HZA+13] is therefore given by $\hat{\mathbf{p}} = E_T(q([1,2,\ldots,K]))$. Hence, the proposed estimator only considers one combination of pairwise error probabilities of the relays to estimate the relay errors.

In order to reduce the estimation variance with the help of the law of large numbers, the estimated relay errors can be calculated as the mean of estimated errors for different permutations of pairwise error probabilities. Hence, an improved estimate $\hat{\mathbf{p}}_i$ is given by

$$\hat{\mathbf{p}}_i = \frac{1}{P_K} \sum_{p=1}^{P_K} E_T(q(P_p(\{1,2,\ldots,K\}))), \tag{3.8}$$

where P_K denotes the number of permutations of K elements, given by $P_K = K!$ and $P_p(\mathscr{K})$ denotes the pth permutation of the set $\mathscr{K}$. The performance improvement of this technique greatly depends on the number available permutations and hence on the number of relays in the network.

Least-Squares Solution of Over-Determined System From the pairwise error probabilities q_{ij}, the proposed algorithm in [HZA+13] solves the following equation system to calculate the relay errors $\hat{p}_i$ with a non-negative constrained least squares solution:

$$q_{12} = \hat{p}_1 + \hat{p}_2 - 2\hat{p}_1\hat{p}_2 \tag{3.9}$$
$$q_{23} = \hat{p}_2 + \hat{p}_3 - 2\hat{p}_2\hat{p}_3 \tag{3.10}$$
$$\vdots \tag{3.11}$$
$$q_{K,1} = \hat{p}_K + \hat{p}_1 - 2\hat{p}_K\hat{p}_1 \tag{3.12}$$

Hence, to calculate K relay errors, K equations and K pairwise estimated errors are considered. However, according to the handshake problem [BK04], $\binom{K}{2}$ different pairwise errors can be estimated and hence be used as input for

Algorithm 1 to estimate the relay errors $\hat{\mathbf{p}}$. With this approach the estimation accuracy can be increased since a least squares solution is found which utilizes the complete information of the system and not only a subset.

3.1.3 Novel Approaches for Pairwise Estimators

This section presents some novel pairwise error probability estimators that are studied with the hope of improving the estimation accuracy compared to the state-of-the-art estimator (3.3). Here, two correlated sequences of LLRs are compared packet-by-packet to estimate the probability of error between the two sequences. Since the decoding process produces error bursts rather than scattered errors, in reality the number of errors between blocks may vary greatly. Thus, the number of samples to use is always limited to the code block length N.

3.1.3.1 Model-Based Unbiased Estimator

Let the estimator input be two sequences of LLRs: $L_1(n)$ and $L_2(n), n = 1,2,...,N$, where N is the code block length in terms of data bits. When obtained directly via Gaussian channel and assuming binary modulation $u_i \in \{\pm 1\}$, the corresponding LLRs can be written as

$$L_i(n) = 2\gamma_i u_i(n) + 2\sqrt{\gamma_i} z_i(n), \quad i = 1,2 \tag{3.13}$$

where γ_i is the per-bit SNR for sequence i, and $z_i(n)$ is a real unit-variance zero-mean Gaussian random variable. Here, the data amplitude or *mean* is $2\gamma_i$, and the *variance* of the noise is $4\gamma_i$. The mean and the variance are connected by the consistency relation *mean* = *variance*$/2$ [Bri01]. We assume that this consistency holds also for post-decoding LLRs, and utilize it in the estimation of q. It is also assumed that γ_i is constant (flat) over each estimation period (code block).

We calculate the powers of and the cross-product between the LLR sequences as

$$P_i \triangleq \frac{1}{N}\sum_{n=1}^{N} |L_i(n)|^2, \quad i = 1,2 \tag{3.14}$$

$$C \triangleq \frac{1}{N}\sum_{n=1}^{N} L_1(n)L_2(n), \tag{3.15}$$

and obtain the statistical properties

$$\mathbb{E}[P_i] = 4(\gamma_i^2 + \gamma_i), \quad i = 1,2 \tag{3.16}$$

$$\mathbb{E}[C] = 4(1-2q)\gamma_1\gamma_2, \tag{3.17}$$

where the pairwise error probability $q \triangleq Pr(u_1(n) \neq u_2(n))$. Now, estimates of the sequence-specific SNRs and of the error probability q can be solved as

$$\hat{\gamma}_i = \frac{1}{2}(\sqrt{P_i + 1} - 1), \quad i = 1,2 \tag{3.18}$$

$$\hat{q} = \frac{1}{2}(1 - \frac{C}{4\hat{\gamma}_1\hat{\gamma}_2}). \tag{3.19}$$

These estimates are unbiased asymptotically, i.e., when N grows large. It can also be seen that the SNR estimates are always non-negative. However, $\hat{q}$ may get negative values as well. The negative values can easily be avoided by truncating negative values to zero.

The model-based estimation is sensitive to the assumptions. If the a-posteriori LLRs from the decoder output turn out not be not consistent, or if the channel (SNR) over the code block is not flat, the estimator performance will degrade.

3.1.3.2 Heuristic Estimators

The simplest pairwise error probability estimator one can think of is "hard" BER counting, where we just calculate how many times $L_1(n)$ and $L_2(n)$ have different signs. At low observation SNR, this kind of estimator is poor due

to the high rate of decision errors in the observed sequences. In this case, the estimator is counting the bit errors caused by the relay-destination channels instead of the underlying errors that were made at the relay. When SNR grows, BER counting will produce accurate results.

As a refinement to the hard BER counting, we introduce "soft" BER counting defined as

$$\hat{q} = \frac{1}{2}\left(1 - \frac{\sum_{n=1}^{N} L_1(n)L_2(n)}{\sum_{n=1}^{N} |L_1(n)L_2(n)|}\right). \tag{3.20}$$

Here, the uncertain samples with low magnitudes get lower weighting in the estimation, while the certain samples with high magnitudes are weighted more. Soft BER is consistent with hard BER in the sense that if all samples have equal magnitude, the two estimators are equal. Furthermore, both hard and soft BER counts get values only between 0 and 1.

3.1.4 Numerical Results of Proposed Estimators

3.1.4.1 Reference Scenario and State-of-The-Art Performance

To investigate the decoding and estimation performance with the proposed estimation algorithms, we consider the CEO system model described in Section 2.2.2 and Figure 2.6 with $K = 7$ relays, where the error probabilities of the BSCs are given by the values in Table 3.1. Each block contains of $N = 1000$ payload bits. Figure 3.4 shows the decoding performance at the destination. There, an AWGN channel is considered, where each channel between the relay and the destination has the provided SNR. Figure 3.4 shows both the decoding performance with known correlation and with the correlation estimated by the SoTA algorithm provided, where $T = 2$. With higher SNR (SNR$> -2.5dB$), the correlation estimation becomes unbiased, but at lower SNR the estimation performance is very inaccurate. Hence, according to the figure, both the waterfall region and error floor can be improved with better correlation knowledge. Accordingly, the waterfall region can be shifted to the left by 1.4dB.

Table 3.1: Bit flipping probabilities for the considered scenario.

k	1	2	3	4	5	6	7
p_k	0.17	0.19	0.03	0.19	0.13	0.02	0.06

The standard deviation of the estimator over several runs is illustrated in Figure 3.5a. As visible, the standard deviation is relatively high compared to the magnitude of the relay errors and hence it is very likely that one relay error is estimated to 0. It is worth to note, that the deviation does not decrease with a higher SNR, instead it seems to be an inherent property of the underlying estimator. The error floor with estimated $\hat{p}_k$ is above the optimal error floor with known correlation. Compared to perfect correlation knowledge, by using a more accurate estimator the error floor can hence be reduced to one third in the presented scenario.

3.1.4.2 Performance of Modified Estimators

This section summarizes the decoding and estimation performance of the algorithm modifications described in sections 3.1.2.1 and 3.1.2.2, based on the pairwise estimator (3.3), in the above scenario. The look-up table for the considered scenario providing the optimal T for the pairwise error estimation is provided in Figure 3.5b. As can be seen, the optimal threshold tends to consider all LLRs for estimation in high SNR regions, but considers only reliable LLRs in worse channel conditions to provide better error estimates. The resulting decoding and estimation performance with the optimized T is shown in Figure 3.6. Compared to Figure 3.4, with the optimized T the error probabilities can be already estimated in lower SNR regimes. Accordingly, the waterfall region of the decoder is shifted to the left, leaving a gap of only $0.4dB$ compared to the ideal curve. However, the error floor remains high and far above the achievable error floor with perfect correlation knowledge.

In order to remove the error floor, singular estimation, i.e. one relay is estimated to have zero error, needs to be combated. This can be done by providing a more accurate solution to the estimation performance, meaning that the estimator's variance is reduced. The standard deviation of the improved estimation algorithms using several

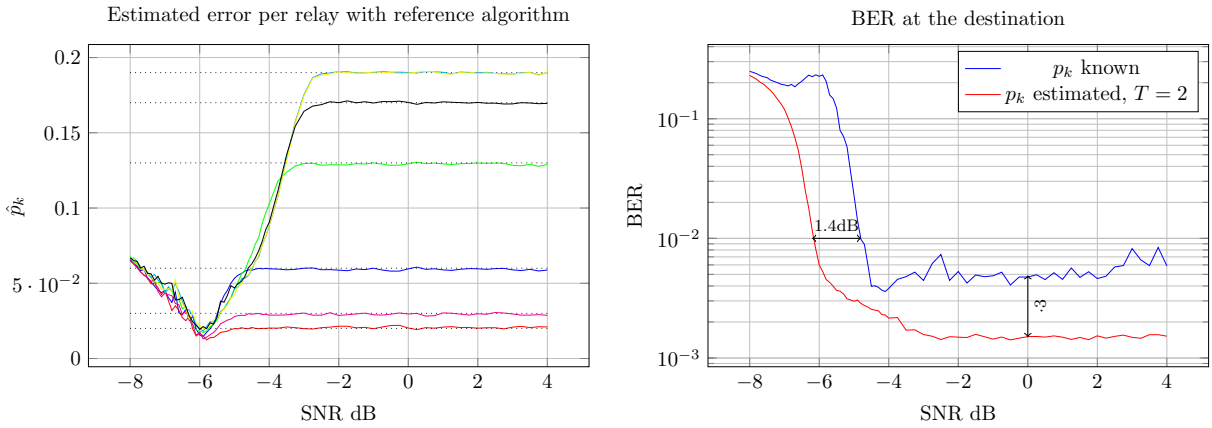

Figure 3.4: Relay error estimation and decoding performance at the destination with reference correlation estimation algorithm and perfect correlation knowledge.

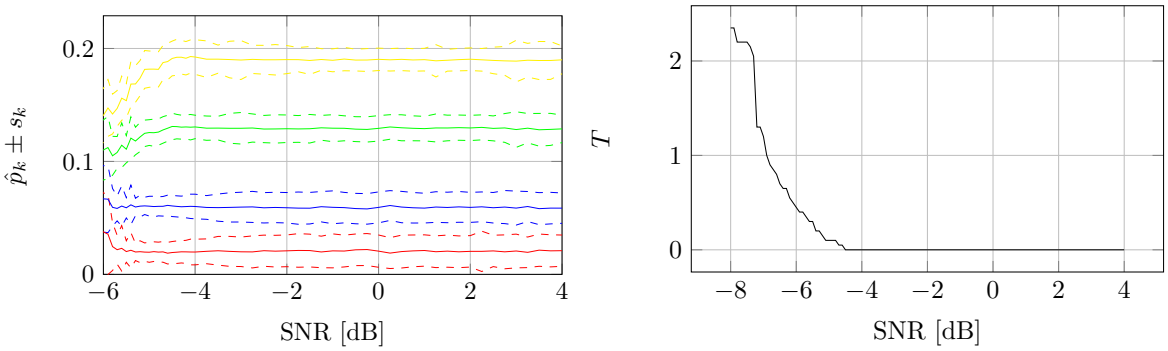

(a) Standard deviation of the estimation performance of the reference estimator [HZA+13] for selected relays with constant $T = 2$.

(b) Look-up table of the optimal T calculated by Algorithm 2.

Figure 3.5: Standard deviation and optimal threshold.

permutations or an overdetermined equation system is shown in Figure 3.7 and numerical values for the resulting standard deviation are shown in Table 3.2, where the standard deviation is averaged over the denoted E_b/N_0 range. Obviously, the estimation performance can be significantly improved by using all available information in the estimator. Furthermore, solving the over-determined system outperforms the permutation approach by 33% reduced standard deviation.

Table 3.2: Standard deviation of modified estimators.

$E_b/N_0 \in [-5dB, 4dB]$	Estimator in [HZA+13]	Permutations	Over-Determination
$\bar{s}_{\hat{\mathbf{p}}}$	$1.3 \cdot 10^{-2}$	$0.34 \cdot 10^{-2}$	$0.19 \cdot 10^{-2}$

The decoding performance at the destination with the correlation estimator which exploits the over-determination of the system is shown in Figure 3.8. The waterfall region is remarkably close to the optimal performance and the error floor is equal to optimal performance. This shows that the improved estimators have significantly improved the overall decoding performance at the destination.

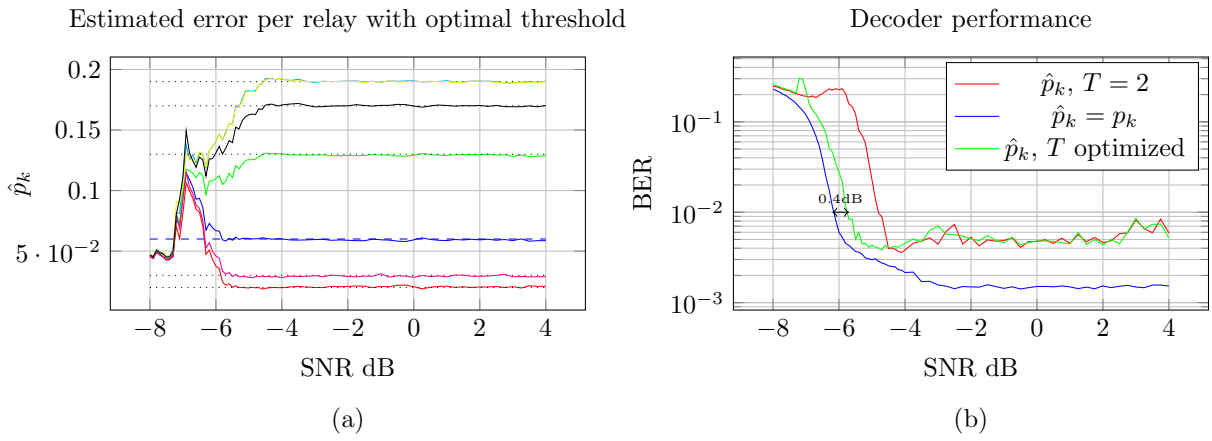

Figure 3.6: Decoding and error estimation performance when using the optimized threshold.

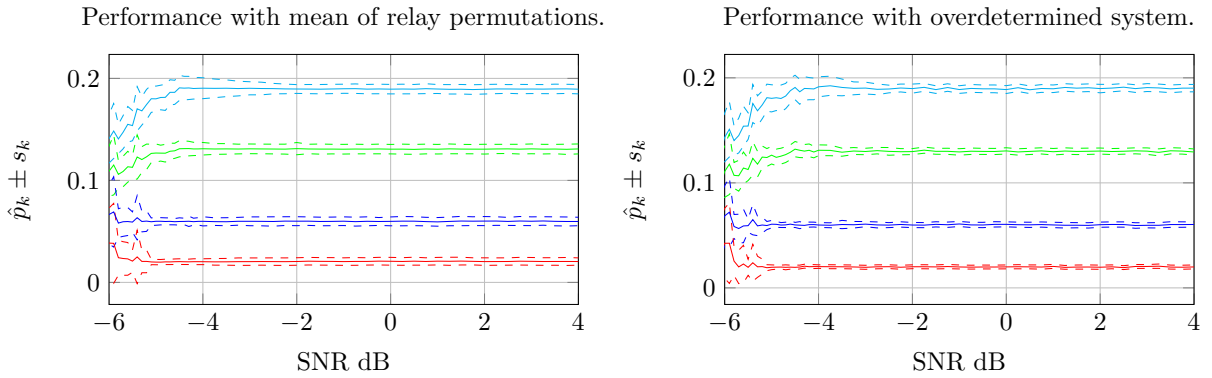

Figure 3.7: Error estimation performance with reduced variance and using optimized threshold.

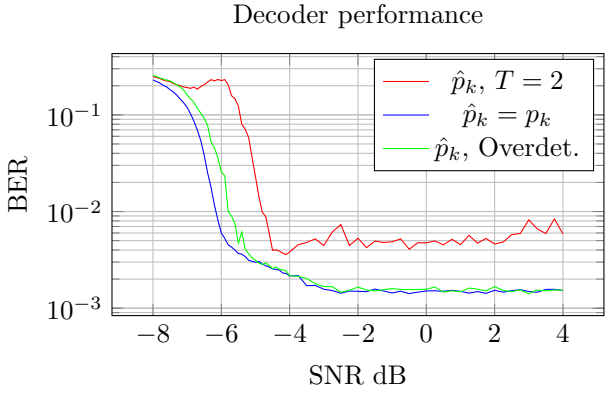

Figure 3.8: Decoding performance at the destination with improved estimator using the overdetermined equation system and optimized threshold.

3.1.4.3 Performance of Novel Pairwise Estimators

The novel pairwise error probability estimators – model-based unbiased, soft BER, and hard BER – presented in Section 3.1.3 were experimented by generating two flat LLR sequences drawn from Gaussian distributions as defined in (3.13). Error probability q was estimated over 10000 randomly generated blocks by different estimators, and the mean and mean-squared-error (MSE) of the estimators was calculated. In addition, a genie-aided nearly optimal threshold setting for the sample selection was experimented. The criterion for the threshold setting was to minimize MSE.

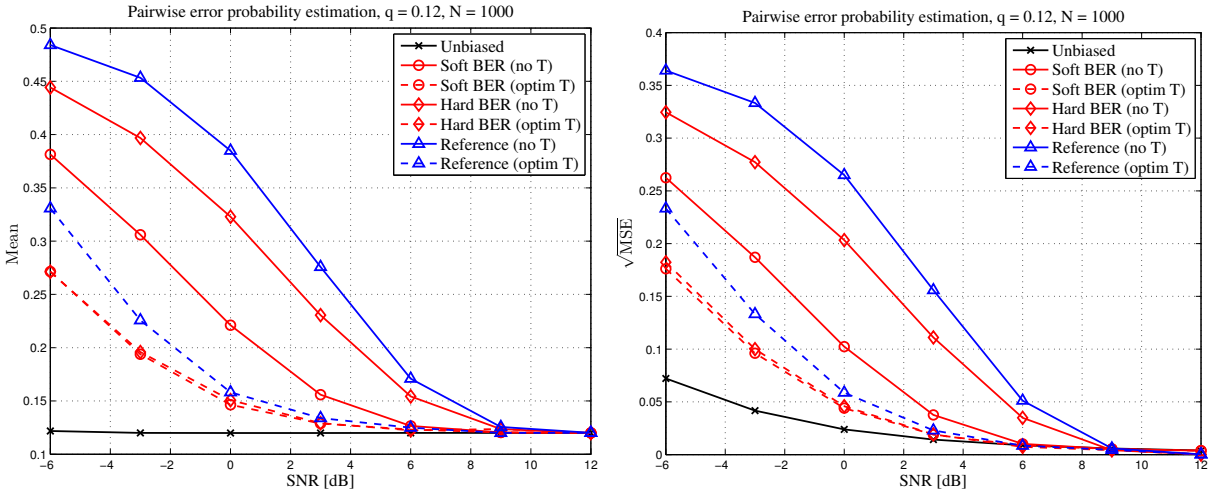

Figure 3.9: Mean and $\sqrt{\text{MSE}}$ of pairwise error probability estimation as function of LLR-SNR, $q = 0.12$, $N = 1000$.

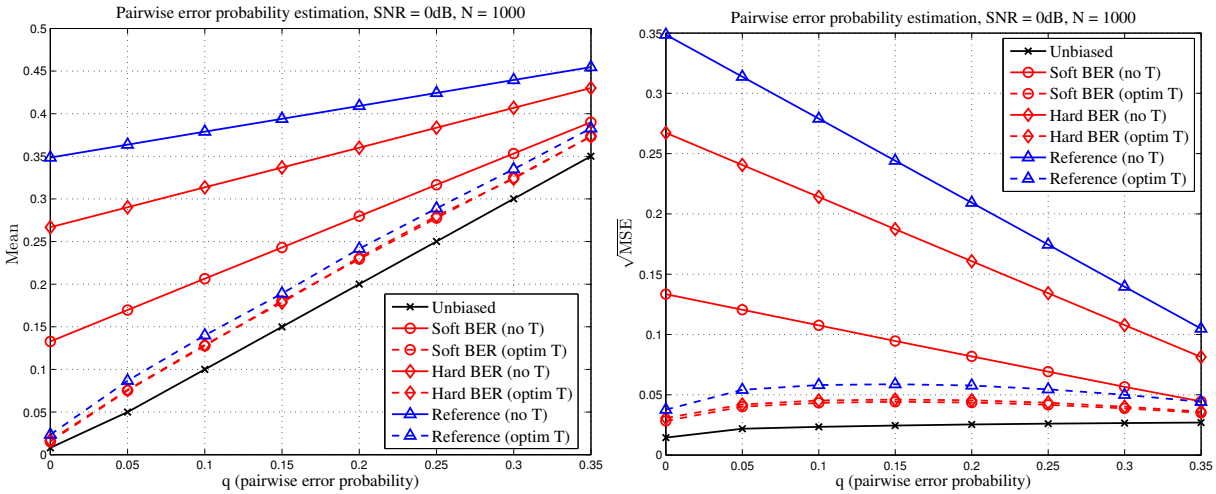

Figure 3.10: Mean and $\sqrt{\text{MSE}}$ of pairwise error probability estimation as function of error probability q, SNR=0dB, $N = 1000$.

The results are shown in Figures 3.9, 3.10, and 3.11. As can be seen, both soft and hard BER perform better than the reference method. Furthermore, the threshold setting reduces bias for all (biased) methods. Adaptive thresholding is also able to benefit from the increasing block length.

The model-based estimator is very accurate and asymptotically unbiased. It relies on the consistency property of the LLRs, and it also assumes that the SNR over each code block is constant (flat). This estimator does not need sample selection or threshold setting: all samples are good samples. The model-based estimator may be sensitive to the breach of the underlying assumptions.

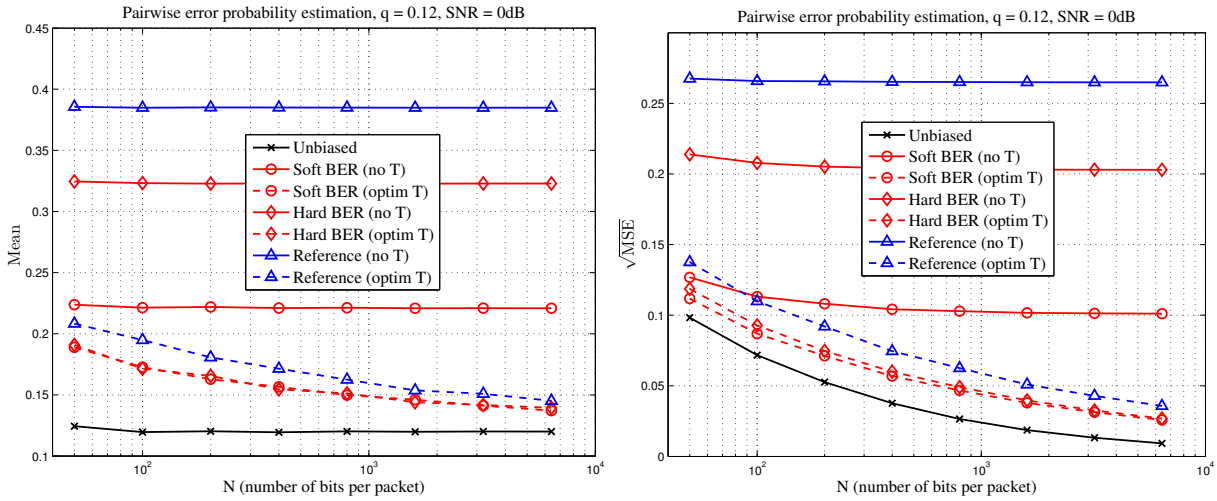

Figure 3.11: Mean and $\sqrt{\text{MSE}}$ of pairwise error probability estimation as function of code block length N, $q = 0.12$, SNR=0dB.

Soft BER counting is not based on any assumptions of the LLR distribution. It is a heuristic refinement to the straightforward hard BER counting. Like the reference method, both soft and hard BER counting schemes can be combined with sample selection to further improve the estimation accuracy.

To investigate the final decoding performance with the novel estimation algorithms, we again simulated the Chief Executive Officer (CEO) system model described in Section 2.2.2 and Figure 2.6 with $K = 7$ relays, where the error probabilities of the Binary Symmetric Channel (BSC)s are given by the values in Table 3.1. The reference least-squares estimator for resolving the underlying BSC error probabilities from the pairwise error probability estimates was used. It turned out that the best decoding performance is obtained when all the LLR samples are used, and thus results only without sample selection are shown here.

Figure 3.12 depicts the decoding performance as a function of the per-link SNR. The results are surprising in the sense that the best performance is achieved by using the simple hard BER counter instead of the more advanced estimators. The model-based unbiased estimator performs clearly worst. There are multiple candidate explanations to this phenomenon. The first is that the distribution of the post-decoding LLRs does not follow the ”consistency condition”, which renders the unbiased estimator almost useless. The second is that the least-squares estimator is more robust when the pairwise error probabilities have been over-estimated, which helps to avoid getting zeros for BER-estimates. The third explanation is that also the iterative decoder actually benefits from over-estimated bit error probabilities, especially in the beginning of the iteration. Clearly, further investigations are needed.

Finally, Figure 3.13 shows a comparison between the SoTA estimator with fixed ($T = 2$) and adaptive threshold setting, over-determined least-squares estimator, and hard BER counting (no sample selection, reference least-squares). As can be seen, even the hard BER counting outperforms the SoTA estimator with fixed T. Due to its reasonable performance and extreme simplicity, hard BER is a potential candidate for implementation.

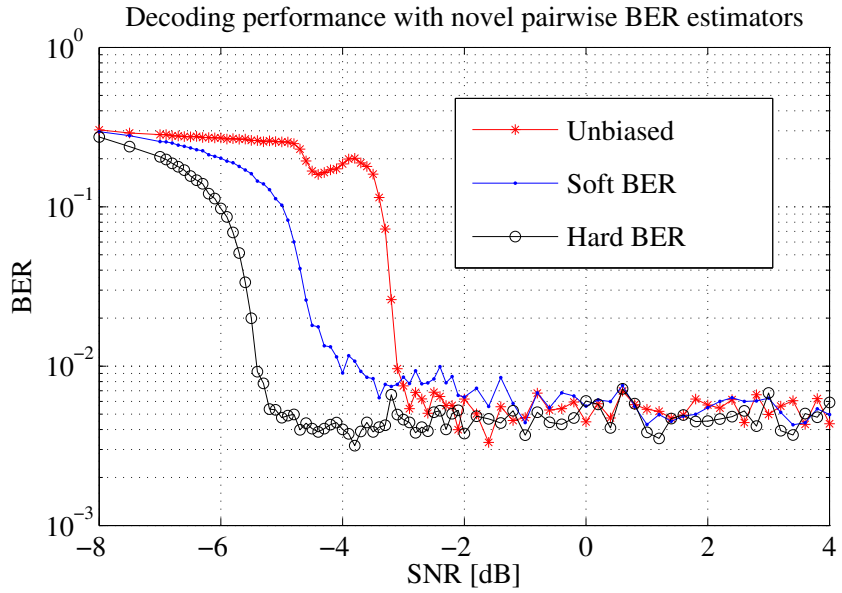

Figure 3.12: Decoding performance with novel pairwise BER estimators, no sample selection ($T = 0$).

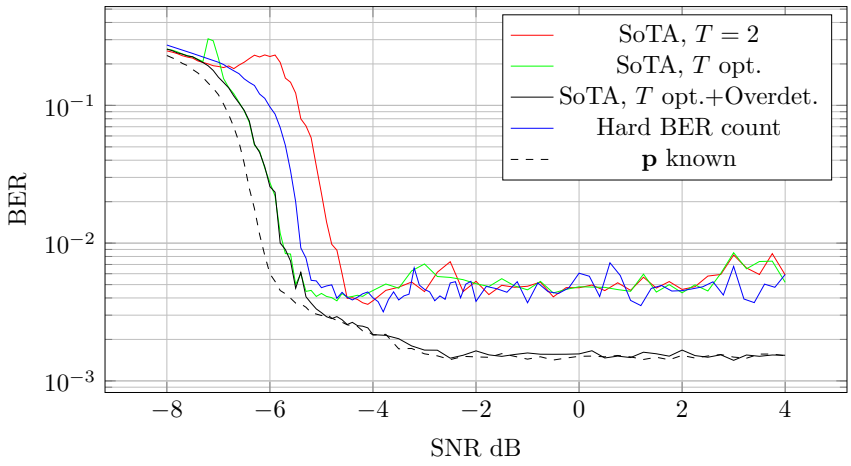

Figure 3.13: Comparison of decoding performance of the proposed estimators.

3.2 Source Correlation Estimation at Relays

In this section, a complexity reduced error-propagation mitigation algorithm is proposed by exploiting limited channel feed-forward from the relay node to the destination node. The proposed idea employs limited channel feed-forward bits as the source-relay correlation information indicator and uses it for the iterative decoding at the destination node. Comparing with the state-of-the-art schemes (i.e. see [AM12a; HZA+13]), the proposed algorithm omits the threshold-based iterative estimation process, and thus the computational complexity at the destination node can be reduced. Also, with limited channel feed-forward, the spectral efficiency of the system can be improved by comparing with the soft-information forwarding scheme. It is shown in the simulations that the proposed algorithm based on limited channel feed-forward can provide a similar performance as the threshold-based estimation algorithm. Moreover, the results also show that the proposed algorithm by exploiting the source-relay correlation information outperforms the conventional selective decode-and-forward (S-DF) relaying up to 1 dB gain by introducing extra decoding process at the destination node.

3.2.1 System Model

The block diagram of the considered single-relay system model is shown in Figure 3.14.

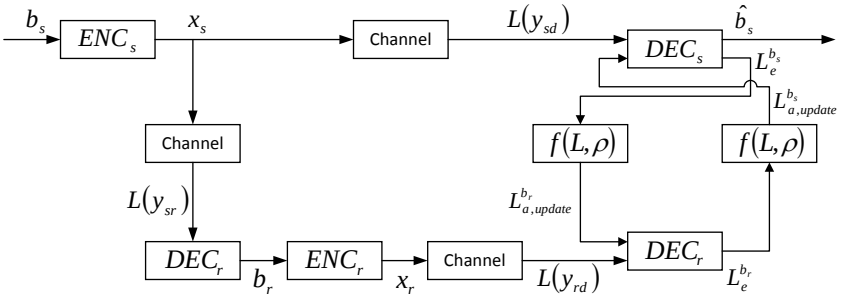

Figure 3.14: The block diagram of the system model.

As shown in the figure, at the source node, the data sequence $\mathbf{b}_\mathrm{s}$ is firstly encoded by the channel encoders ENC_s using turbo principle, and then modulated by binary phase shift keying (BPSK) to obtain the modulated sequence $\mathbf{x}_\mathrm{s}$. After that, $\mathbf{x}_\mathrm{s}$ is transmitted to the relay node and the destination node in time-slot 1. As follows, the recovered binary sequence $\mathbf{b}_\mathrm{r}$ at the relay node is encoded by the turbo encoders ENC_r and modulated by BPSK to generate the signal sequence $\mathbf{x}_\mathrm{r}$. $\mathbf{x}_\mathrm{r}$ is then forwarded to the destination node during time-slot 2. After receiving the signals from the source node and the relay node, the destination node performs joint turbo decoding by exploiting the correlation information to retrieve the original data sequences from the source node. Here, the message $\mathbf{b}_\mathrm{r}$ which is obtained by the relay node is the erroneous version of the original data sequences $\mathbf{b}_\mathrm{s}$. Thus, the binary data sequences emitted from the source node and the relay node are correlated with each other. The correlation information can be expressed as [AM12a]

$$\rho = 1 - 2p_e, \tag{3.21}$$

where $p_e = \Pr(b_\mathrm{s} \neq b_\mathrm{r})$ is the error probability of the corresponding bit between the source node and the relay node, and it is in a range of $[0, 0.5]$.

3.2.2 The Source-Relay (S-R) Correlation Knowledge Estimation

As mentioned in Sec. 3.2.1, the destination node performs joint turbo decoding by exploiting the correlation information to retrieve the original data sequences from the source node. Such decoding process can be found in [AM12a]. It was shown in [AM12a], when p_e is unknown at the destination node, the threshold-based estimation method (i.e. see [GZ05]) can be implemented to obtain the p_e value. Here, the threshold is imposed to limit the number of log likelihood ratio (LLR) values for calculation to guarantee the estimation reliability. The estimation accuracy mainly depends on the threshold set-up. If the threshold is set up to a very big value, few LLR values can meet the requirement and N will approach to 0. If the threshold is set up to a very small value, a lot of unreliable LLR values will be included in the estimation process and the accuracy of p_e estimation cannot be

guaranteed. Thus, the main drawback of the threshold-based estimation method is that biased estimation results may be produced when different threshold values are applied.

Motivated by the above observation, a novel scheme to exploit the channel state information (CSI) of S-R link to obtain the correlation information p_e (also ρ) is proposed. As we know, the p_e value is an indication of the channel quality of S-R link. When transmission over quasi-statistic fading channels, the block-wise constant fading coefficient and the power of additive white gaussian noise (AWGN) determine the received signal-to-noise ratio (SNR) for each transmitted block, which can be used to link with the p_e value at the relay node. According to this, a look-up table then can be built up in order to link different SNRs with different p_e values. Such look-up table needs to be shared by both the relay node and the destination node before data transmission. Then, at the relay node, after obtaining its estimated SNR value, it can search the look-up table to find the corresponding p_e value and then forward the corresponding index to the destination node. With such procedure, at the destination node, the p_e value can be obtained based on the feed-forward index bits, and thus, the p_e estimation can be omitted.

Table 3.3: Look-up table for p_e with channel information, where the SNR thresholds are corresponding to the p_e obtained through S-R link training.

SNR range	p_e level	SNR range	p_e level
(-∞ , -14.5]	0.463	(-4.5,-3.5]	0.167
(-14.5, -10.5]	0.432	(-3.5,-2.5]	0.117
(-10.5,-9.5]	0.328	(-2.5,-1.5]	0.0429
(-9.5, -8.5]	0.308	(-1.5, -0.5]	0.00821
(-8.5, -7.5]	0.287	(-0.5,0.5]	0.000282
(-7.5,-6.5]	0.263	(0.5,1.5]	0.00000123
(-6.5,-5.5]	0.236	(1.5, +∞)	0.000
(-5.5, -4.5]	0.205		

Table 3.3 gives an example of different SNR ranges corresponding to different average p_e values. The look-up table pre-stores the average p_e values for different CSI ranges, and an indicator symbol is used to represent the SNR ranges with their corresponding average p_e values, e.g., a 4-bit symbol to present 16 SNR ranges and their corresponding average p_e values. In order to formulate the different average p_e values for different SNR ranges of S-R link, an off-line training is designed by employing the low complexty decoding algorithm at the relay node through the non-fading AWGN channel. It is worthwhile to note that, if a relatively strong code is used and the block-length is long, the threshold-based estimated results converge to the average error probability, especially at a high SNR range. Thus, the channel information is able to provide a relatively accurate estimation on p_e.

3.2.3 Performance Analysis

3.2.3.1 Convergence Property

Figure 3.15 and Figure 3.16 compare the proposed p_e estimation scheme with the threshold-based p_e estimation scheme in terms of the p_e performance and the mean square error (MSE) performance, respectively. Assume that the SNR of S-R link is fixed to -2 dB, hence, for the proposed p_e estimation scheme, based on the above look-up table 3.3, the estimated average p_e value in this case is equal to 0.0429. For the threshold-based p_e estimation scheme, different thresholds are set up for the p_e estimation. Turbo-like codes are used for encoding/decoding process, where each encoder at both source node and relay node is an non-recursive convolutional code with a generator polynomial $G = ([6, 13])_8$, the decoding process at the relay node is only with 2 horizontal iterations, and the decoding precess at the destination node is with 5 horizontal iterations and 5 vertical iterations. As shown in Figure 3.15, the estimated p_e values of the threshold-based p_e estimation scheme decreases as the SNR of source-destination (S-D) link increases, and finally they are converged to the estimated average p_e value of the proposed p_e estimation scheme when the SNR of S-D link is above 0 dB. In Figure 3.16, the MSE performance of the threshold-based p_e estimation scheme also converges to the ones of the proposed p_e estimation scheme as the SNR of S-D link increases. Furthermore, the convergence rate of the threshold-based p_e estimation scheme depends on the value of the threshold set-up, since the threshold affects the number of samples and the reliability of the p_e estimation. It is shown that, as the reliability of the decoding process increases (e.g. the SNR value of S-D link increases), the estimation accuracy of the threshold-based p_e estimation scheme increases. In contrast,

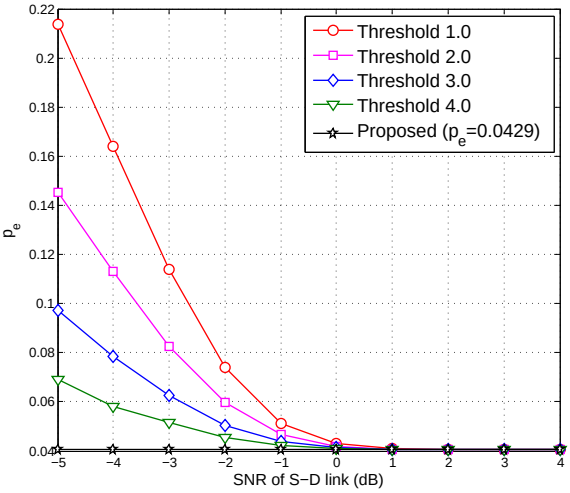

Figure 3.15: The threshold-based estimation of p_e with various threshold set-ups and block-length=1000.

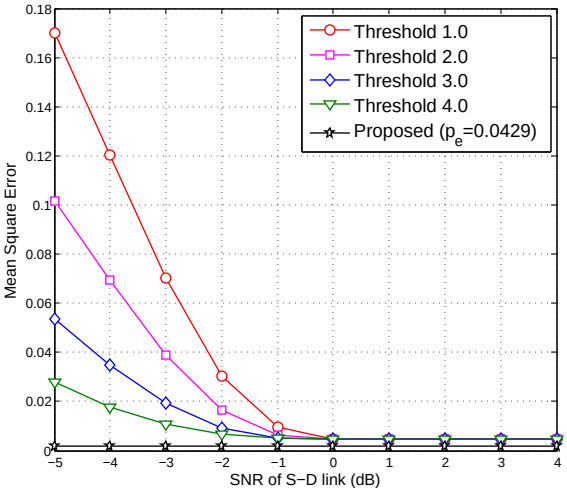

Figure 3.16: MSE of estimation p_e with various threshold set-ups and block-length=1000.

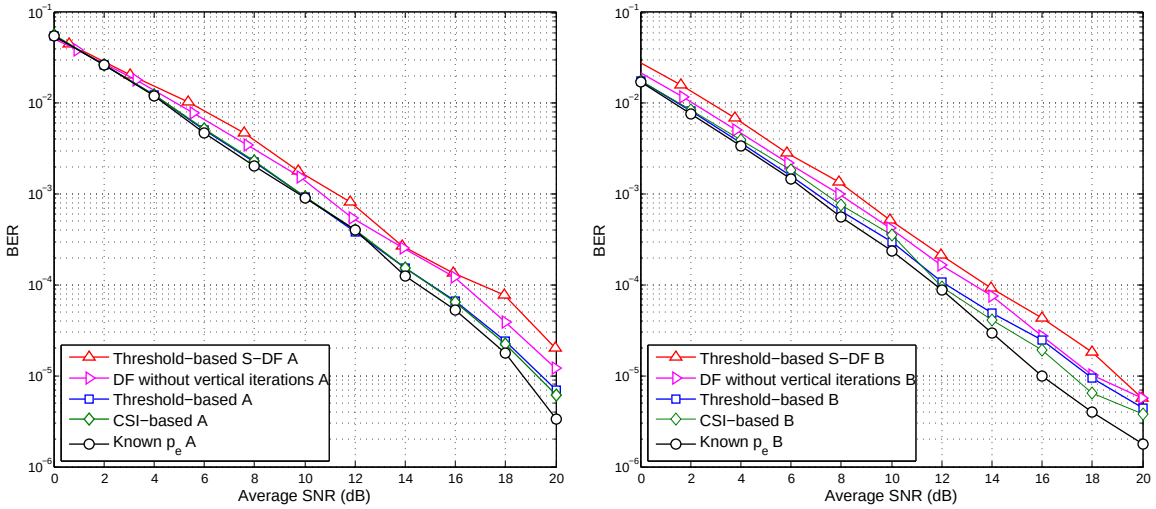

Figure 3.17: BER performance in block Rayleigh fading channels and block-length=1000.

for the proposed channel feed-forward scheme, the correlation information can be accurately obtained regardless of the channel quality of S-D link and the threshold set-up.

3.2.3.2 BER Performance

Figure 3.17 illustrates the bit-error-rate (BER) performance of the schemes exploiting correlation information compared with conventional S-DF relaying. For the S-DF relaying, two methods are used to control the error propagation. One is using a cyclic redundancy check (CRC) at the relay node, where the relay node remains silence if the CRC fails. The other one is SNR threshold-based check, where the relay node only operates when the SNR of S-R link exceeds a predetermined value. In this experiment, the same turbo-like code as last experiment is used, the block-length is set up to 1000 bits, and 10000 blocks are transmitted from the source node. For the threshold-based S-DF relaying, an 1-dB SNR threshold is employed to control the error propagation at the relay node. The relay node is placed in two positions: A) in the middle of the S-D link, which results a 6 dB SNR gain for S-R link and relay-destination (R-D) link comparing to the S-D link; B) in the position where the distance of S-R and R-D links are the same as that of S-D link. To demonstrate the performance gain achieved by exploiting the S-R link correlation, the BER curves of conventional S-DF relaying are provided as the benchmark. The performance

of threshold-based p_e estimation at the destination scheme is also presented, where the threshold is set to 2.0. The ideal scenario with known p_e at the destination node is used as the upper bound for comparison. It can be observed that the proposed scheme exploiting CSI-based correlation information at the relay node can achieve 1 dB gain over the conventional S-DF relaying schemes at BER of 10^{-4}. Moreover, it is also found that the BER curve of the proposed scheme is very close to that of the ideal situation using actual p_e and the threshold-based p_e estimation scheme, which means that the complicated iterative p_e estimation process at the destination node can be replaced by the limited channel feed-forward at the relay node, thus, the computational complexity at the destination node can be significantly reduced.

3.2.4 Summary

In this section, a novel strategy for iterative decoding exploiting correlation information with limited channel feed-forward at the relay node has been presented. The proposed algorithm aims to mitigate the error propagation at the destination node through the limited channel feed-forward of S-R link correlation information from the relay node. Here, a look-up table is used to provide the S-R link channel correlation information. It is shown that the proposed scheme can outperform the conventional S-DF relaying scheme. Moreover, without the p_e estimation process at the destination node, the proposed scheme can achieve close BER performance as the scheme that the p_e is estimated at the destination node.

3.3 Summary and Discussion

In order to optimally decode received messages, the proposed joint decoder requires the knowledge of correlation information between the relays. However, if all relays experience some errors, the joint decoder will always have a decoding error floor since it can happen that all relays have made an error for the same bit. To acquire knowledge about the correlation, the decoder can estimate the bit errors at the destination by considering the decoded LLRs. The estimation is carried out in three phases: 1) The LLR samples that are used for estimation are selected. This can either be done by thresholding or using the some percentile of the most reliable LLRs. 2) Pairwise bit errors between relays are estimated. 3) The pairwise bit errors are used to resolve the actual transmitter-specific BER. In this chapter new methods for all three phases were presented. It is worth mentioning that in order resolve the transmitter-specific BERs at the destination – based on just the pairwise estimates – at least three transmitters, or at least three different packet copies, need to be received.

In the estimation, each received code block (packet) is treated separately, which takes into account the fading state of the channel and the decoding success per block. For each packet, the correlation between messages is newly analyzed to get most accurate results. Hence, the estimation complexity needs to be considered in the overall system complexity. Therefore, in comparison to the conventional estimator, a new promising low-complexity pairwise BER estimator based on the hard BER count was presented. It showed slightly worse performance compared to the higher complexity estimators based on threshold adaptation that were proposed in this chapter.

An alternative approach to obtain the correlation knowledge for the destination is to estimate the BER already at the relays by measuring the channel state of the source-relay link. The BER information can then be forwarded to the destination, however here quantization noise and signaling overhead appears. The BER estimation at the relays is especially useful, when there are error-free relays. Error-free relays can hardly be estimated at the destination as a wrong singular estimation can significantly influence the decoder error floor. In addition, CRC checks at the relays can help in finding the zero BER packet copies. Forwarding the CRC pass or fail information would only require one bit signaling overhead but can potentially improve performance significantly. One more estimation strategy could be to consider the decoded LLRs at the relays. This approach would provide soft information of the decoding success of each packet separately, whereas the CRC check can only resolve whether the packet is totally error-free or not.

It is worth noting that most of the studied estimators assume that SNR per link can be accurately estimated to calculate the BER or to adjust the sample selection threshold. This assumption is not restrictive as channel state and noise variance information is necessary also for running the iterative turbo decoding process itself. Finally, as estimates are always in practice inaccurate, the estimates provided by the relays could be further improved by utilizing pairwise BER estimation methods at the destination in conjunction with the iterative decoder. It is

certainly a future design challenge to find a protocol that provides the best trade-off between decoding performance, estimation complexity, and signaling overhead.

4. Advanced Topologies and Access Methods

In this chapter, complex communication network structures such as multi-route relaying with more than two hops, and relaying with multiple source transmitters are addressed. The specific problems are described, coding and decoding solutions presented, and performance results shown. Furthermore, the concept of IDMA is motivated and explained, the related additional functionality at the receiver is described, and numerical results are shown.

4.1 Interleave-Division Multiple-Access (IDMA)

In our previous work, orthogonal transmission is assumed to be used for multiple relays when transmitting messages to the common destination. In order to keep the transmissions orthogonal, different time slots are required for different relays. Interleave-division multiple-access (IDMA) technique [FOO00; LVW+06] can be applied here for the transmissions of relays to reduce the number of required time slots while still maintaining good system performance. IDMA technique is somewhat similar to code-division multiple-access (CDMA) technique, and the two system models are shown in Fig. 4.1. IDMA uses different interleavers to separate the users, while CDMA uses spreading codes. The key idea of IDMA is that the interleaver plays a role of user identification without using spreading, and hence, we can allocate the entire bandwidth expansion to coding by using very low-rate codes with the aim of achieving the optimal multiple access channel (MAC) capacity and maximizing the coding gain [VS99]. Hence, designing very low-rate codes is a crucial problem in IDMA systems in order to maximize the coding gain.

In order to approach the MAC capacity, multi-user detection (MUD) should be performed at the receiver. A sub-optimal but simpler approach is to employ single-user detection (SUD), and accept some reduction in the achievable rates. In this section, we review the code design, SUD, MUD as well as the BER performance evaluation of the IDMA technique [WAM14].

4.1.1 Code design

The motivation of using concatenated single parity check and irregular repetition (SPC-IrR) codes together with extended mapping (EM) in IDMA systems is threefold: 1) very low-rate can be achieved using SPC-IrR codes, as stated above, designing low-rate codes is a very important issue in IDMA; 2) the code design is flexible using EXIT-constrained binary switching algorithm (EBSA) [FOT+12]; 3) EM gains additional degree-of-freedom in the system design since the labeling pattern in EM can be easily adjusted.

Fig. 4.2 shows the proposed coding/decoding scheme for IDMA. The information sequence $\mathbf{u}_k = [u_k(i), u_k(2), \cdots, u_k(n)]$ generated by k-th user is first encoded by the SPC-IrR code with coding parameter d_c, d_v and a. A simple example of SPC-IrR code is depicted in Fig. 4.3. The coded sequence $\mathbf{c}_k$ is then permutated by interleaver Π_k and doped-accumulated by ACC with doping ratio p_d. Finally, the output sequence $\mathbf{d}_k$ from ACC is modulated by EM and transmitted to the destination through MAC. Hence, the received signal $\mathbf{r}$ at the destination

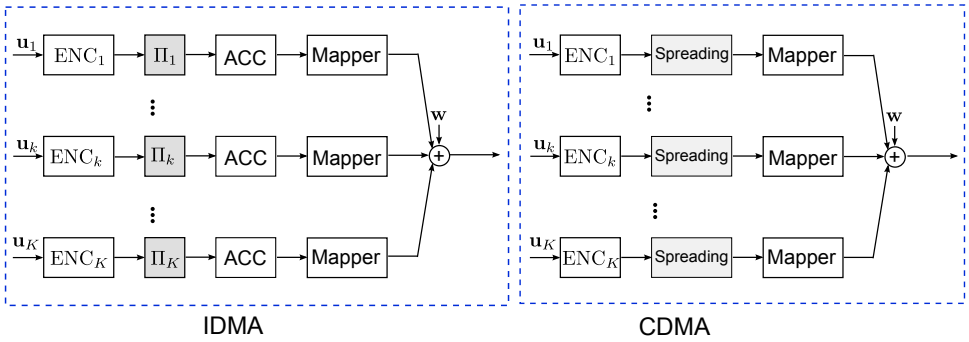

Figure 4.1: A comparison of system models of IDMA and CDMA.

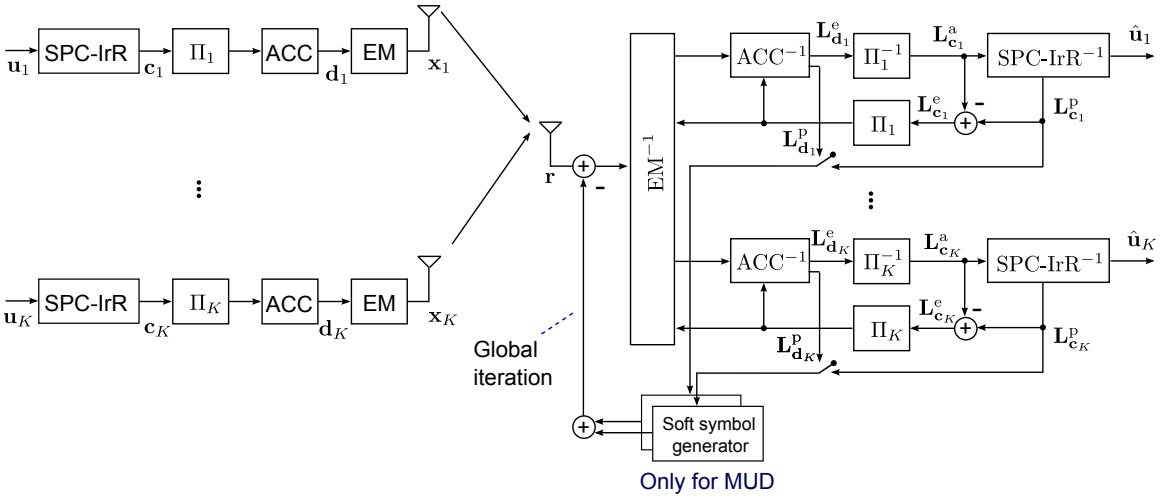

Figure 4.2: System model of the proposed coding scheme and detection algorithm.

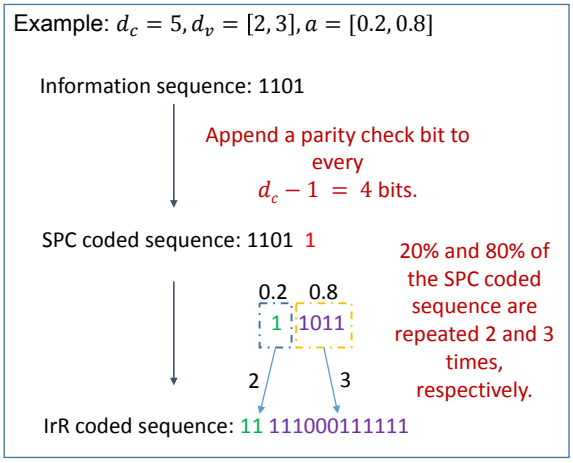

Figure 4.3: A simple example of SPC-IrR code.

is expressed as

$$\mathbf{r} = \sum_{k=1}^{K} \sqrt{P_k} \cdot \mathbf{x}_k + \mathbf{w}, \tag{4.1}$$

where P_k and $\mathbf{w}$ denote the power allocated to the k-th user and the zero mean AWGN sequence with variance σ_w^2, respectively. The source information is then reconstructed from $\mathbf{r}$ based on SUD or MUD we proposed. The details of SUD and MUD is shown in below subsections.

4.1.2 Single-User Detection (SUD)

In SUD, the signals of other users is treated as noise when the k-th user's signal is detected, i.e., the global iteration shown in Fig. 4.2 is not activated. Hence, (4.1) can be rewritten as

$$\mathbf{r} = \sqrt{P_k} \cdot \mathbf{x}_k + \zeta_k, \tag{4.2}$$

with

$$\zeta_k = \sum_{g=1, g\neq k}^{K} \sqrt{P_g} \cdot \mathbf{x}_g + \mathbf{w}, \tag{4.3}$$

where ζ_k indicates the multiple access interference (MAI) from the other users plus AWGN. It is assumed that ζ_k in (4.2) can be approximated as a Gaussian random variable according to the central limit theorem. Thus, the

variance of interference plus noise, experienced by the k-th user, $\sigma^2_{k,\zeta}$, is expressed as

$$\sigma^2_{k,\zeta} = \sum_{g=1,g\neq k}^{K} P_g + \sigma^2_w, \tag{4.4}$$

where we assume $\mathbb{E}[|x_{g,i}|^2] = 1$ with $x_{g,i}$ is the i-th element of $\mathbf{x}_g$. The performance of the SUD reception is interference limited since $\sigma^2_{k,\zeta}$ remains non-zero even if σ^2_w is reduced to zero.

The *extrinsic* information exchange between EM^{-1} and decoder is performed iteratively, at the receiver side, adhering the turbo principle. The *extrinsic* LLR output from the EM^{-1} is fed into the decoder ACC^{-1} to generate the *a posteriori* LLR $\mathbf{L}^{\text{p}}_{\mathbf{d}_k}$ and the *a priori* LLR $\mathbf{L}^{\text{e}}_{\mathbf{d}_k}$. Then the extrinsic LLR $\mathbf{L}^{\text{e}}_{\mathbf{d}_k}$ is deinterleaved and result in *a priori* LLR $\mathbf{L}^{\text{a}}_{\mathbf{c}_k}$, which is input to the decoder SPC-IrR^{-1}. The extrinsic LLR $\mathbf{L}^{\text{e}}_{\mathbf{c}_k}$ output from the decoder SPC-IrR^{-1} is then interleaved and fed back to both ACC^{-1} and EM^{-1}. This process is performed iteratively until no more relevant gain in mutual information can be achieved. Finally, the estimation $\hat{\mathbf{u}}_k$ is obtained based on hard decision of the *a posteriori* LLR of the decoder.

4.1.3 Multi-User Detection (MUD)

The major difference between SUD and MUD is that soft successive interference cancellation (SSIC) [CCC00] is performed in MUD to cancel the interference from the other users. In order to perform SSIC, the global iteration shown in Figure 4.2 is activated in MUD.

The received signal $\mathbf{r}$ is expressed by (4.1)–(4.3) in the same way as in SUD. However, for cancelling out the interference from the other users when we detect the k-th user's signal by SSIC, the received signal r_i is subtracted from the mean value of $\zeta_{k,i}$ as

$$\hat{r}_{k,i} = r_i - \mathbb{E}[\zeta_{k,i}], \tag{4.5}$$

with i representing the symbol index. Now the major task of the "Soft symbol generator" box shown in Fig. 4.2 is to compute the second term of (4.5) to perform SSIC in each global iteration. As stated above, since we assume that $\zeta_{k,i}$ follows Gaussian distribution, the mean and the variance of $\zeta_{k,i}$ is expresses as

$$\begin{aligned} \mathbb{E}[\zeta_{k,i}] &= \mathbb{E}[\sum_{g=1,g\neq k}^{K} \sqrt{P_g}\cdot x_{g,i} + w_i] \\ &= \sum_{g=1,g\neq k} \sqrt{P_g}\cdot \mathbb{E}[x_{g,i}], \end{aligned} \tag{4.6}$$

where $\mathbb{E}[x_{g,i}]$ represents the mean value of g-th user's i-th soft symbol. $\mathbb{E}[x_{g,i}]$ can be calculated in each global iteration based on the *a posteriori* LLR sequence $\mathbf{L}^{\text{p}}_k = \mathbf{L}^{\text{p}}_{\mathbf{c}_k} + \mathbf{L}^{\text{p}}_{\mathbf{d}_k}$ fed back from the decoder, as

$$\mathbb{E}[x_{k,i}] = \sum_{s\in S} s \prod_{\varpi=1}^{\ell} P(d_{k,\varpi} = W), \tag{4.7}$$

with

$$P(d_{k,\varpi} = W) = \frac{\exp(-d_{k,\varpi} L^{\text{p}}_{k,\varpi})}{1+\exp(L^{\text{p}}_{k,\varpi})}, \tag{4.8}$$

where $W \in \{0,1\}$ and ϖ is bit index of i-th EM symbol. S is a set of constellation points with s representing its element. However, for initialization, the mean $\mathbb{E}[x_{g,i}]$ is set to 0.

Since SSIC is performed, the variance σ^2_{k,ζ_i} of $\zeta_{k,i}$ is also updated by (4.9) and used in EM^{-1} to calculate the extrinsic LLR in each iteration.

$$\sigma^2_{k,\zeta_i} = \sum_{g=1,g\neq k}^{K} P_g \cdot \sigma^2_{g,x_i} + \sigma^2_w, \tag{4.9}$$

with

$$\sigma^2_{g,x_i} = \mathbb{E}[|x_{g,i} - \mathbb{E}[x_{g,i}]|^2]. \tag{4.10}$$

The initial value of σ^2_{g,x_i} is set to 1 to activate the global iteration. The process of SSIC and decoding is iteratively performed until the required iteration times are reached.

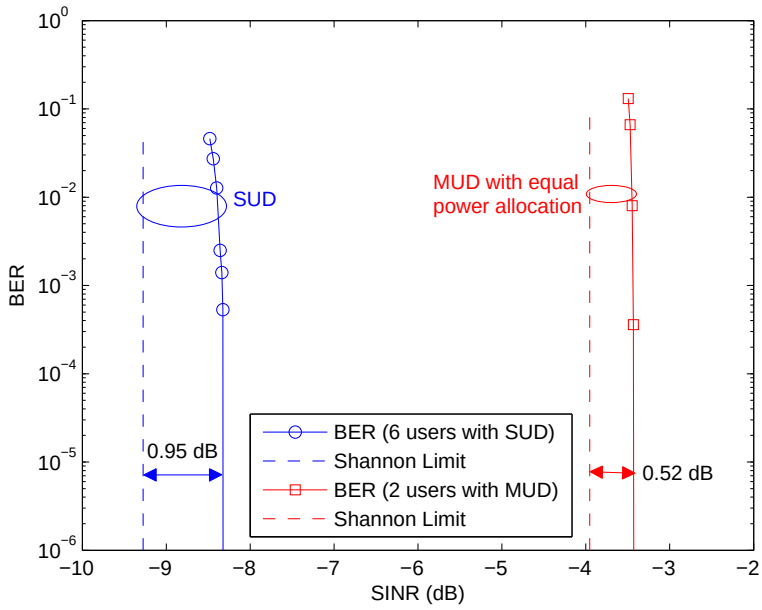

Figure 4.4: BER performance of IDMA-SUD and IDMA-MUD with equal power allocation. The coding parameters are: $d_c = 5, d_v = [2,5,20,21,100], a = [0.0721, 0.2441, 0.4767, 0.1610, 0.0461], p_d = 10$ **for SUD, and** $d_c = 5, d_v = [2,6,7,23,24], a = [0.2542, 0.2479, 0.436, 0.0109, 0.0511], p_d = 20$ **for MUD. The coding rates are 0.0424 and 0.1226 for SUD and MUD, respectively [WAM14].**

4.1.4 Numerical Results

With the proposed coding/decoding scheme in IDMA system, good BER performance versus SINR can be achieved with SUD, where the SINR of k-th user $SINR_k$ is defined as

$$SINR_k = \frac{P_k}{\sum_{g=1,g\neq k}^{K} P_g + \sigma_w^2}. \tag{4.11}$$

The BER performance with SUD is shown in Fig. 4.4. It can be found that the BER at 10^{-5} range is only around 0.95 dB away from the Shannon limit. However, when the number of users increases, BER versus each user's SINR, degrades due to the multiple access interference from the other simultaneous users. Therefore, to achieve better performance, a technique to reduce or to ultimately eliminate the interference, such as SSIC, is needed.

The BER performances with MUD is also shown in Fig. 4.4. With our proposed technique, the BER threshold is very sharp and no error-floor is visible in the BER range. Due to the exactly matched EXIT curves combined with the soft cancellation technique, very near-capacity performance, only $\{0.52\}$ dB away from the corresponding limit, is achieved.

However, the BER performance is degraded when equal power is allocated to users in MUD. We can further improve the system performance by using unequal power allocation scheme, which is shown in [WAM14].

4.2 Coding and Decoding for Multi-Hop Relaying

In our previous work, we assume that the signal of single hop relays can cover the distance between the source and the destination. However, if the destination and the source is far away, we should also establish effective lossy forwarding techniques for this case. This motivates us work on multi-hop relaying system using lossy forwarding relays. Recently, multi-hop relaying networks have been recognized as an effective technique to increase the coverage of signals. In a multi-hop network, a source and a destination exchange information through a set of relays which are located in different hops, and hence, the source can transmit its information to the destination

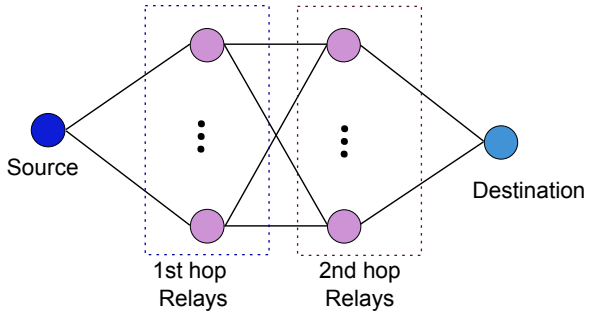

Figure 4.5: A schematic diagram of a two-hop relaying system with cross-link transmission.

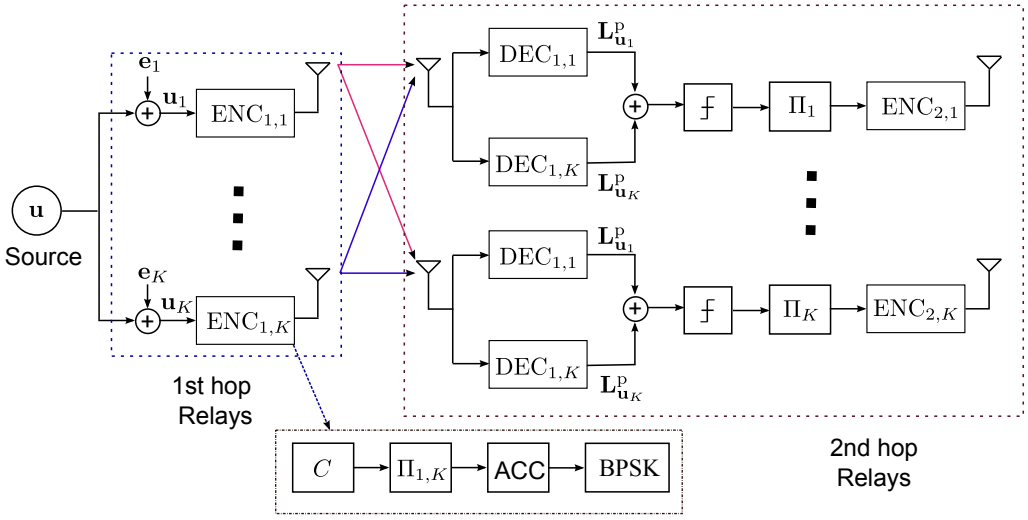

Figure 4.6: The proposed coding scheme for the two-hop relaying network.

via different routes connected by relays. In [SLW+09], authors proposed and analyzed several novel solutions including separation of control and data, effective SINR-based routing as well as cooperative relay schemes in order to improve both the system capacity and coverage. A suboptimal path selection based on using amplify-and-forward (AF) protocol at relays was proposed in [YLR+12], with the target of achieving outage probability close to that of the optimal routing scheme. The outage probability of using maximum distance separable code at link-level cooperative multi-hop relaying network was evaluated in [SIT10]. However, in this section, we study a multi-hop relaying network using decode-and-forward (DF) protocol at relays and evaluate the BER performance.

4.2.1 System Model: Coding and Decoding

We consider a two-hop relaying system where a schematic diagram is shown in Fig. 4.5 to examine the lossy forwarding technique we proposed.

Figure 4.6 shows the proposed coding scheme for a two-hop relaying network to be analyzed. A binary i.i.d. source $\mathbf{u} = [u(1), u(2), \cdots, u(i), \cdots, u(n)]$ is transmitted to multiple relays at the first hop, where i is the time index and n represents the block length. For simplicity, we assumed the channels between the source and the relays at the first hop are simply BSCs. The received message $\mathbf{u}_k$ of k-th relay is then a corrupted version of $\mathbf{u}$ by the binary error sequence $\mathbf{e}_k$ with $\Pr(e_k(n) = 1) = p_k$, where $k = 1, 2, \cdots, K$ indicates the index of relays. Consequently, the messages at relays are correlated with each other since they have the common input $\mathbf{u}$ of the independent BSCs. The k-th relay encodes the message $\mathbf{u}_k$ by an encoder C and then interleaves the encoder output by $\Pi_{1,k}$. The interleaved information is then doped and accumulated by the ACC. Finally, the output of the ACC is modulated by BPSK and transmitted to all the relays at the second hop over AWGN channels. We currently assume that the transmissions are orthogonal with each other to ensure interference-free reception. In order to guarantee orthogonal transmission, different time slots are allocated to the transmission. However, we can use IDMA technique for non-orthogonal transmission to reduce the number of time slots, which is left as future work in our next stage.

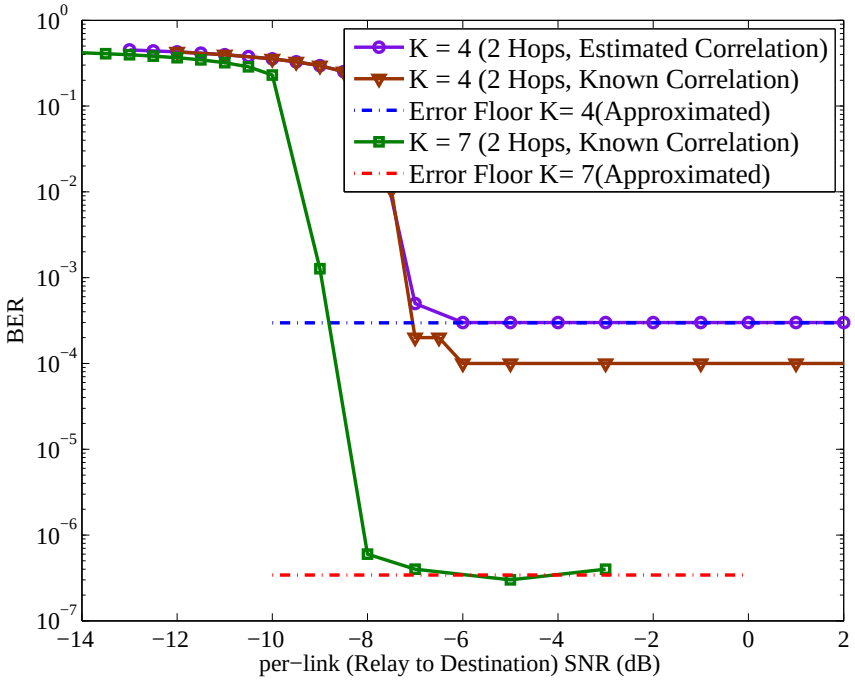

Figure 4.7: The BER performance of our proposed scheme.

The k-th relay at the second hop first decodes the signal received from each relay at the first hop with a few iterations L. The estimate $\hat{\mathbf{u}}_k$, which is generated based on the hard decision for the summation of the posteriori LLRs $\mathbf{L}^{\mathrm{p}}_{\mathbf{u}_k}$, is first interleaved by an random interlaver Π_k and then encoded by using the same coding chain as that using by the relays at the first hop. After that, the modulated signal is transmitted to the destination over independent AWGN channel.

The proposed decoding algorithm at the destination is shown in Figure 2.7, which is the same as we have proposed in [HZA+13] for the binary data gathering WSN, and hence, we have not provided the detail description of the decoding algorithm used in this section.

4.2.2 Results and Discussion

The BER performances are evaluated by running a series of simulations. The obtained results are shown in Figure 4.7 with different numbers of relays K at each hop as a parameter. The parameters were set as follows:

- Block length $n = 10000$ bits.
- Interleavers: random.
- Encoder C: rate $R^{\mathrm{c}}_k = \frac{1}{2}$ nonrecursive systematic convolutional code with generator polynomial $G = [03, 02]_8$.
- Doping ratio of the ACC: 1.
- Crossover probability of BSCs: 0.01.
- The number of iterations at the second hop: 1.
- Decoding algorithm for D and ACC^{-1}: log-maximum *a posteriori* (MAP).
- The number of iterations at the destination: 25 times of GI and LI.
- SNR_{rr} representing the per-link SNR from relays to relays was set larger than SNR_{rd} representing the per-link

SNR from relays to the destination by δ (dB). We set $\delta = 8$ for $K = 4$ and $\delta = 15$ for $K = 7$.

From the simulation results from Figure 4.7, it is found that the BER of the two-hop relaying network can also have a very sharp turbo cliff and the same level of error floor as in the single hop relaying network. It should be noted here that the errors in the information sequence obtained at the second hop relays after hard decision are correlated with each other. This is the key reason that we can not get better error floor in multi-hop relaying system than the single-hop relaying system. Furthermore, the power allocation is extremely important to achieve such good performance in this two-hop relaying network. If the power of the relays at the first hop is too low, the BER performance may degrade a lot since the correlation among the signals received at the destination becomes very small. Therefore, in the simulations, we set the SNR_{rr} larger than SNR_{rd}, however, this is not the optimal allocation of power. In our future work, the optimal power allocation and/or rate allocation in multi-hop relaying networks in order to achieve minimal BER performance will be carried out by using convex optimization tools.

4.3 Joint Adaptive Network and Channel Coding for Orthogonal Multiple Access Relay Channel

4.3.1 System Model

Figure 4.8 illustrates a basic model of the orthogonal multiple access relay channel (MARC) system allowing intra-link errors (MARC-IE), where there are two source nodes A and B, a single relay R, and one common destination D. The N-bit length i.i.d. binary information sequences generated from nodes A and B are denoted as $\mathbf{u}_A = \{u_A(k)\}_{n=1}^N$ and $\mathbf{u}_B = \{u_B(k)\}_{n=1}^N$, respectively. The signaling scheme used at the source node is denoted as $\mathscr{E}_S(\cdot)$, which consists of a serial concatenation of channel encoding and modulation.

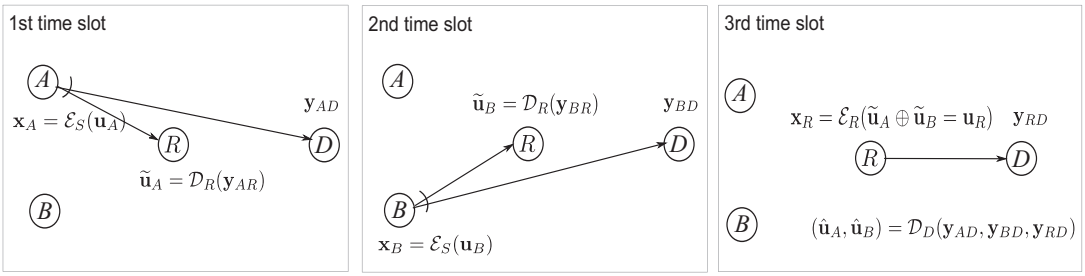

Figure 4.8: Orthogonal MARC-IE system model, where there are three time slots in a transmission cycle [LZM14].

There are three time slots in one transmission cycle. In the first two time slots, nodes A and B respectively broadcast their M-bit length coded sequences $\mathbf{x}_A = \mathscr{E}_S(\mathbf{u}_A) = \{x_A(m)\}_{m=1}^M$ and $\mathbf{x}_B = \mathscr{E}_S(\mathbf{u}_B) = \{x_B(m)\}_{m=1}^M$ to R and D, and their corresponding received signals obtained at R and D are respectively written as

$$\begin{aligned} \mathbf{y}_{iR} &= h_{iR} \cdot \mathbf{x}_i + \mathbf{n}_{iR} \\ \mathbf{y}_{iD} &= h_{iD} \cdot \mathbf{x}_i + \mathbf{n}_{iD}, \qquad i \in \{A, B\} \end{aligned} \tag{4.12}$$

where h_{iR} and h_{iD} indicate the channel coefficients of iR and iD links with the source node i, respectively. $\mathbf{n}_{iR}$ and $\mathbf{n}_{iD}$ indicate the vectors of independent zero-mean complex additive white Gaussian noise (AWGN) of the iR and iD links, respectively, with variance $\sigma_{iR}^2 = \sigma_{iD}^2 = \sigma^2$ per dimension. The iR and iD links are also referred to as the intra and direct links, respectively, in this section.

The receiver applied at the relay R is denoted as $\mathscr{D}_R(\cdot)$, composed of signal detection and decoding, which corresponds to the inverse structure of $\mathscr{E}_S(\cdot)$. The estimates $\widetilde{\mathbf{u}}_i = \mathscr{D}_R(\mathbf{y}_{iR})$ of $\mathbf{u}_i$ obtained at R may contain errors due to the variation of the iR link. The error probability of the iR link is represented by

$$p_i = \mathfrak{B}(\mathbf{u}_i, \widetilde{\mathbf{u}}_i) = \frac{\sum_{n=1}^N |u_i(n) - \widetilde{u}_i(n)|}{N}, \quad i \in \{A, B\}. \tag{4.13}$$

In the orthogonal MARC system with selective decode-and-forward relaying strategy (MARC-SDF) [IH11], if the estimates $\widetilde{\mathbf{u}}_i$ is found to contain errors, it will be discarded at the relay. However, in the proposed MARC-IE system model, the estimates $\widetilde{\mathbf{u}}_A$ and $\widetilde{\mathbf{u}}_B$, are always joint network-channel coded at R regardless of whether they are correct or not, as

$$\mathbf{x}_R = \mathscr{E}_R(\mathbf{u}_R) = \mathscr{E}_R(\widetilde{\mathbf{u}}_A \oplus \widetilde{\mathbf{u}}_B) = \{x_R(m)\}_{m=1}^{M}, \tag{4.14}$$

where the notation $\oplus$ denotes a binary exclusive-OR (XOR) operation and $\mathscr{E}_R(\cdot)$ represents the signaling scheme applied at R, including channel encoding and modulation. In the second time slot, the destination D receives the signal vector $\mathbf{y}_{RD}$ of $\mathbf{x}_R$ sent via the relay-destination (RD) link as

$$\mathbf{y}_{RD} = h_{RD} \cdot \mathbf{x}_R + \mathbf{n}_{RD}, \tag{4.15}$$

where h_{RD} and $\mathbf{n}_{RD}$ indicate the channel coefficient and AWGN vector with variance $\sigma_{RD}^2 = \sigma^2$ of the RD link, respectively. The estimates of $\mathbf{u}_R$ obtained at the destination is denoted as $\hat{\mathbf{u}}_R$, and the error rate of the RD link is $p_R = \mathfrak{B}(\mathbf{u}_R, \hat{\mathbf{u}}_R)$. Finally, to obtain the estimates $\hat{\mathbf{u}}_A$ and $\hat{\mathbf{u}}_B$ of the information sequences $\mathbf{u}_A$ and $\mathbf{u}_B$, respectively, at the destination, decoding of JNCC is performed on the received signal vectors $\mathbf{y}_{AD}$ and $\mathbf{y}_{BD}$ with the help of the signal vector $\mathbf{y}_{RD}$.

Following the block Rayleigh fading assumption, h_{iR}, h_{iD} and h_{RD} are assumed to be constant over one coded sequence but vary independently transmission-by-transmission and link-by-link. Without loss of generality, we assume that $E[|h_{iR}|^2] = E[|h_{iD}|^2] = E[|h_{RD}|^2] = 1$. The error probabilities p_i and p_R, thus, vary in each transmission cycle. The instantaneous SNRs γ_{iR}, γ_{iD} and γ_{RD} of the links are then given by

$$\begin{aligned} \gamma_{iR} &= |h_{iR}|^2 \cdot \Gamma_{iR}, \\ \gamma_{iD} &= |h_{iD}|^2 \cdot \Gamma_{iD}, \\ \gamma_{RD} &= |h_{RD}|^2 \cdot \Gamma_{RD}, \end{aligned} \tag{4.16}$$

where Γ_{iR}, Γ_{iD} and Γ_{RD} represent the average SNRs of the intra, direct and RD links, respectively.

4.3.1.1 Network Correlation

The errors occurring in the two SR links can be described by the bit-flipping model with flipping probability $p_i,\ i \in \{A,B\}$. Then, since XOR-network coding is always performed at the relay in the proposed MARC-IE system, we found a new bit-flipping probability p_{nc} between the two sequences: one is the forwarded XOR-coded sequence $\mathbf{u}_R$ generated at the relay (i.e., $\mathbf{u}_R = \widetilde{\mathbf{u}}_A \oplus \widetilde{\mathbf{u}}_B$, and the other is their corresponding XOR-ed information sequences $\mathbf{u}_\oplus$ (i.e., $\mathbf{u}_\oplus = \mathbf{u}_A \oplus \mathbf{u}_B$). Hence, the probability p_{nc} between original two XORed information $\mathbf{u}_\oplus$ and $\mathbf{u}_R$ can be calculated as

$$\begin{aligned} p_{nc} &= \Pr(\mathbf{u}_R \neq \mathbf{u}_\oplus) \\ &= \Pr((\widetilde{\mathbf{u}}_A \oplus \widetilde{\mathbf{u}}_B) \neq (\mathbf{u}_A \oplus \mathbf{u}_B)) \\ &= 1 - (1-p_A)(1-p_B) - p_A p_B \\ &= p_A + p_B - 2 \cdot p_A p_B. \end{aligned} \tag{4.17}$$

We refer the probability p_{nc} as network correlation. Note that although p_{nc} is assumed to be known to the destination in this section, p_{nc} can also be estimated at the destination using the estimation methods presented in Section 3.1. In the following subsection, we will show how the network correlation p_{nc} can be utilized in the joint decoding process at the destination to help recover the original information sequences $\mathbf{u}_A$ and $\mathbf{u}_B$.

4.3.2 Coding and Decoding Scheme

4.3.2.1 Coding Structure at The Source and Relay Nodes

The key idea with MARC-IE system is that the relay always performs XOR coding on $\widetilde{\mathbf{u}}_A$ and $\widetilde{\mathbf{u}}_B$ to obtain $\mathbf{u}_R$, and then the interleavered version of $\mathbf{u}_R$ is encoded and modulated with $\mathscr{E}_R(\cdot)$. In summary, the coding structures at the

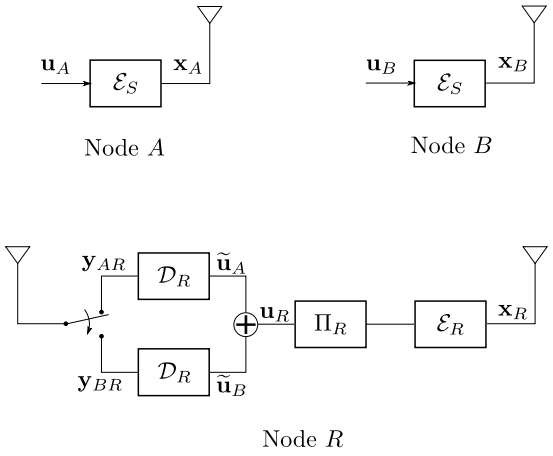

Figure 4.9: Coding structures at the source and relay nodes for proposed MARC-IE.

source and relay nodes are illustrated in Figure 4.9.

We use the same coding chain for both $\mathscr{E}_S$ and $\mathscr{E}_R$, which is a serial concatenation of a half-rate recursive convolutional code (RSC) with generator polynomial $(07,05)_8$ and a accumulator (ACC), followed by BPSK modulation. As a consequence, the spectrum efficiency of both $\mathscr{E}_S$ and $\mathscr{E}_R$ are $1/2$. All the interleavers used are random interleavers. Note the receiver $\mathscr{D}_R$ at the relay simply extracts the original information by performing hard-decision on the output from the differential detection. This greatly reduces the computational complexity at the relay because of its simplicity.

4.3.2.2 Joint Network-Channel Decoding Structure

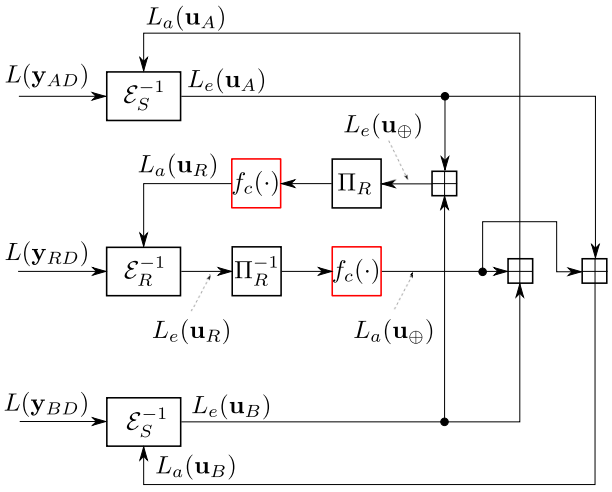

Figure 4.10: Joint network/channel decoding structure for proposed MARC-IE.

The block diagram of the joint network/channel decoding algorithm for the proposed MARC-IE system is shown in Figure 4.10. To utilize the network correlation p_{nc}, the LLR-updating function $f_c(\cdot)$ shown in Equation (2.4) is used in the decoding scheme.

The received signal vectors $\mathbf{y}_{iD}$ from the two source nodes are respectively demodulated at D to obtain the corre-

sponding soft channel values, as

$$L(\mathbf{y}_{iD}|\mathbf{x}_i) = \frac{2}{\sigma^2} \cdot \Re\{\mathbf{y}_{iD} \cdot h_{iD}^*\}, \quad i \in \{A,B\}, \tag{4.18}$$

where the notations $L(\cdot)$ and $\Re(\cdot)$ denote LLR vector and a function that takes the real part of its argument element-wisely, respectively, and $*$ indicates complex conjugation. The computation from received vector $\mathbf{y}_{RD}$ to $L(\mathbf{y}_{RD}|\mathbf{x}_R)$ also applies (4.18). Given these soft channel value vectors, the *extrinsic* LLR vector $L_e(\mathbf{u}_i)$ and $L_e(\mathbf{u}_R)$ are calculated by the soft-in-soft-out (SISO) decoder $\mathscr{E}_S^{-1}(\cdot)$ and $\mathscr{E}_R^{-1}(\cdot)$, respectively, using the Log-MAP algorithm. Then, since XOR-network-coding is performed at the relay, the *extrinsic* LLR vector $L_e(\mathbf{u}_\oplus)$ before the function $f_c(\cdot)$ is obtained by performing the "box-plus" operation [HOP96] bit-wisely on $L_e(\mathbf{u}_A)$ and $L_e(\mathbf{u}_B)$, as

$$L_e(\mathbf{u}_\oplus) = L_e(\mathbf{u}_A) \boxplus L_e(\mathbf{u}_B) = \ln \frac{\exp(L_e(\mathbf{u}_A)) + \exp(L_e(\mathbf{u}_B))}{1 + \exp(L_e(\mathbf{u}_A) + L_e(\mathbf{u}_B))}. \tag{4.19}$$

We then use the function $f_c(\cdot)$ with the knowledge of p_{nc} to obtain the *a priori* LLR values for $\mathbf{u}_R$ by modifying $L_e(\mathbf{u}_\oplus)$, as

$$L_a(\mathbf{u}_R) = f_c\left(\Pi_R\left[L_e(\mathbf{u}_\oplus)\right], p_{nc}\right), \tag{4.20}$$

where $\Pi_R[\cdot]$ denotes interleaving by Π_R. Similarly, we extract $L_e(\mathbf{u}_A)$ and $L_e(\mathbf{u}_B)$ from $L_e(\mathbf{u}_R)$ generated from $\mathscr{E}_R^{-1}(\cdot)$ with the bit-wise "box-plus" operation, and modify them by taking into account the network correlation p_{nc} to obtain *a priori* LLR values for $\mathbf{u}_A$ and $\mathbf{u}_B$ as

$$L_a(\mathbf{u}_A) = f_c(\Pi_R^{-1}[L_e(\mathbf{u}_R)], p_{nc}) \boxplus L_e(\mathbf{u}_B), \tag{4.21}$$

and

$$L_a(\mathbf{u}_B) = f_c(\Pi_R^{-1}[L_e(\mathbf{u}_R)], p_{nc}) \boxplus L_e(\mathbf{u}_A), \tag{4.22}$$

respectively, where $\Pi_R^{-1}[\cdot]$ indicates de-interleaving from Π_R.

4.3.3 Numerical Results

In this subsection, we show the FER performance of the proposed MARC-IE, where all the links in MARC are assumed to suffer from block Rayleigh fading. Two different scenarios are considered: in Symmetric case, the distances from B to R and D are the same with that from A to R and D, respectively; in Asymmetric case, B is further away form R and D than A. The average SNRs of all the links in both scenarios are summarized in Table 4.1, where X represents the average SNR of the AD link in dB; Δ and L denoting additional gain and loss due to the shorter and longer distance, respectively, and are set to 3 dB and 10 dB. In the simulations, the length of information sequence is set at $N = 2048$ bits. The local decoding of $\mathscr{E}_S^{-1}$ is performed 10 iterations, followed by 1 iteration of decoding between $\mathscr{E}_S^{-1}$ and $\mathscr{E}_R^{-1}$, and in total the whole process is repeated 10 times.

Results of the FER performances of the proposed MARC-IE in Symmetric and Asymmetric scenarios are demonstrated in Figure 4.11, where the FER performances of MARC-SDF using the same coding structure are also provided for comparisons. Here FER is defined as follows: number of the transmission cycles where either one or both of the information sequences sent from the nodes A and B cannot successfully recovered at D even with the help of R, divided by the total number of transmission cycles.

Table 4.1: Settings of symmetric and asymmetric scenarios.

Scenario	Γ_{AD}	Γ_{BD}	Γ_{AR}	Γ_{BR}	Γ_{RD}
Symmetric	X	X	X+Δ	X+Δ	X+Δ
Asymmetric	X	X-L	X+Δ	X+Δ-L	X+Δ

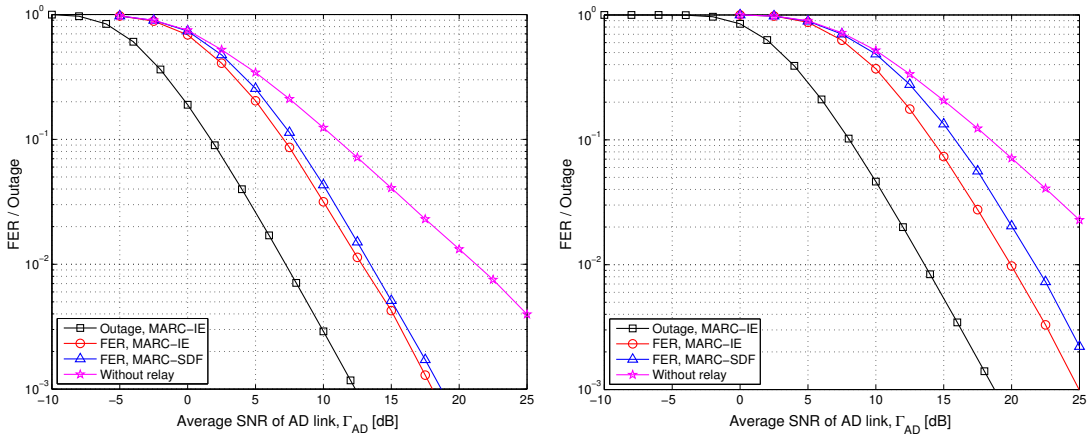

(a) Symmetric scenario (b) Asymmetric scenario

Figure 4.11: FER performances of proposed MARC-IE in Symmetric and Asymmetric scenarios, where all links in MARC suffer from block Rayleigh fading [LZM14].

It can be observed in Figure 4.11 that in Symmetric and Asymmetric scenarios, the proposed MARC-IE respectively obtains 0.7 dB and 2.2 dB gain from the MARC-SDF. This indicates that even though the estimates $\widetilde{\mathbf{u}}_i$ contains errors, the erroneous estimates received at the relay, instead of being discarded, can still be efficiently utilized in the proposed MARC-IE system for reconstructing the information sequences $\mathbf{u}_i$, sent via the *iD* link, at the destination.

The outage probabilities of MARC-IE in both scenarios are also included in Figure 4.11 for reference, which are obtained in [LZM14]. It can be observed from Figure 4.11 that the FER performances of the proposed MARC-IE are roughly 6 dB and 5 dB away from the limits, respectively. It is expected the gap can be narrowed by using capacity-achieving codes and better decoding strategy at the relay.

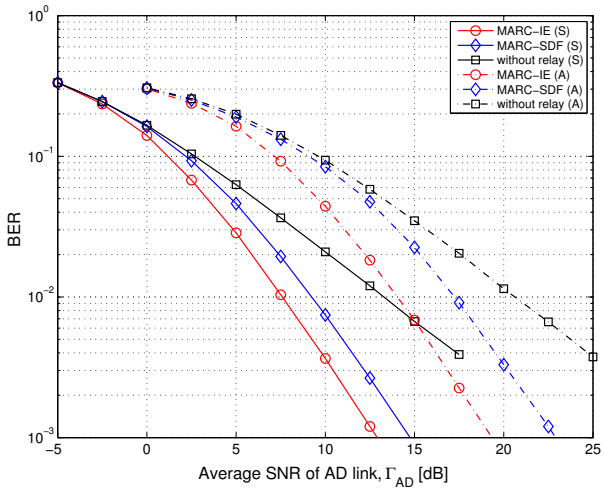

Figure 4.12: BER performances of the proposed MARC-IE, where all links in MARC suffer from block Rayleigh fading.

The BER performances of the proposed MARC-IE and the MARC-SDF systems are demonstrated in Figure 4.12. Compared with the FER performance shown in Figure 4.11, the proposed MARC-IE is more advantageous in BER performance, and provides roughly 2.3 dB and 3.8 dB gain over MARC-SDF at BER = 10^{-3} in Symmetric and Asymmetric scenarios, respectively. This is because with the less amount of mutual information, caused by larger value of p_{nc}, is still possible to correct several error bits, even though it is not enough to correct all the error bits.

5. Support for System Design

This chapter discusses the options for multi-rate coding for the RESCUE system, and the preliminary code design choices for the SDR implementation are disclosed. The basic interfaces between the higher layer protocols and the physical layer coding/decoding are also described. For the purpose of system level simulations, a novel abstract "black box" simulation tool is outlined.

5.1 Multi-Rate Coding

The ability to adjust transmission rate in response to the communication application requirements or wireless channel capacity, is typically realized via multi-rate coding and modulation. To this end, for each supported transmission rate, the code, modulation constellation, and modulation mapping are to be designed.

In the context of turbo codes, a design tool called "EXIT-Constrained Binary Switching Algorithm" (EBSA) has been proposed in [FOT+12]. It is used for finding a good match in terms of EXIT curves between concatenated single parity check and irregular repetition (SPC-IrR) codes and extended mapping (EM). As a result, a wide range of rates can be flexibly supported. The BER performance for various code rates when employing 16QAM modulation are shown in Figure 5.1. It can be seen that excellent BER performance in terms of very sharp turbo cliff can always be achieved.

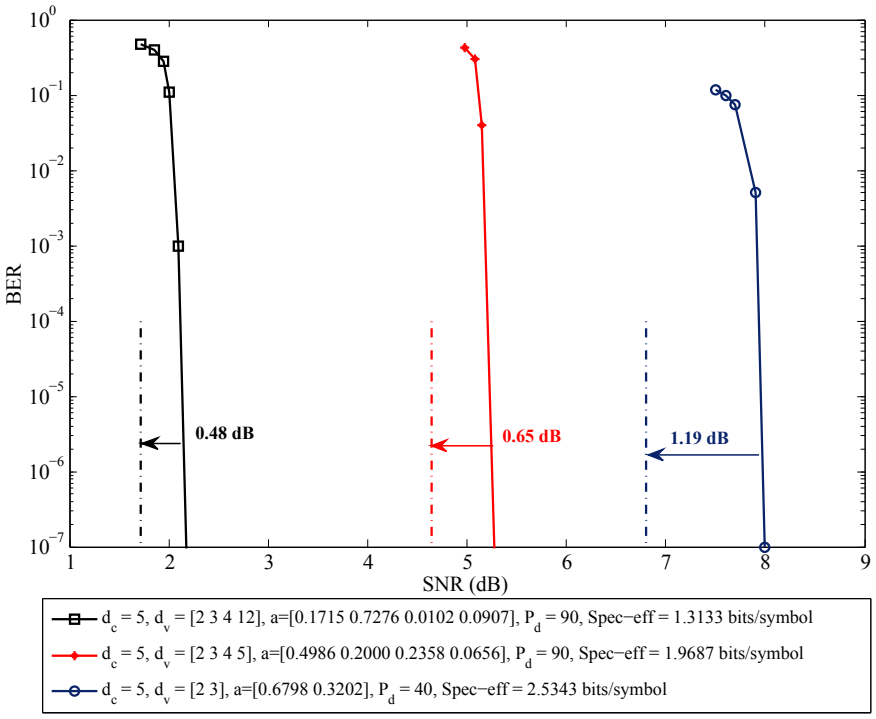

Figure 5.1: The BER performance of the SPC-IrR codes with optimized code parameters and labeling patterns. Spec-eff represents spectrum efficiency.

For the SDR implementation, the emphasis of the multi-rate code design, however, is in simplicity. Our choice for the component code is a rate 1/2 systematic non-recursive convolutional code concatenated with a doped accumulator. The multi-rate functionality is realized via selecting between QPSK and 16QAM modulation schemes. Simple Gray mapping for the modulation is used. This coding scheme is a safe choice as it is known to perform well in the context of multi-rate relaying. However, the choice lacks in flexibility when compared to the approach with SPC-IrR codes and EBSA.

5.2 Interaction with Higher Layers

This section summarizes how the code and decoder design carried out in WP2 interfaces with the work of WP3 and WP4. Section 5.2.1 presents the functional block diagram of the chosen encoding and decoding chain at a relay node. Furthermore, the parameters that need to be signalled or known by the higher layers are shown. In Section 5.2.2, a new abstraction of the physical layer coding functionality, for the purpose of simulating the higher layer protocols such as ARQ and MAC, is proposed.

5.2.1 Functional Block Diagram and Interfaces

The basic functional blocks of the physical layer coding/decoding, and the interfaces towards the higher layer protocols are exemplified in Figure 5.2, where a simplified model of the relay node is depicted. As can be seen, the coding and modulation parameters (modulation and coding set, MCS) for both the received and for the corresponding transmitted packet copy need to be exchanged with higher layers. Most importantly, the interleaving (IL) patterns are different for different transmitting nodes, even if all the other parameters are relatively fixed.

It is recognized that the robust and flexible approach for appropriately signaling the code parameters is to attach a physical frame header carrying the MCS and IL indexes to each of the packet copies at the transmitter side. This way, any receiving node – relay or destination – is able to decode the packet and restore the original payload data. In addition to the code parameters, the header will carry a unique message identifier that enables the receiver to identify which packet copies are to be iteratively combined. However, while it is tolerated that decoding results for the data may be incomplete and include errors, the physical frame headers must always be received without error. Otherwise the decoding process of the data cannot be started. Thus, the physical frame header needs to be well protected by a strong code and/or adequate transmit energy.

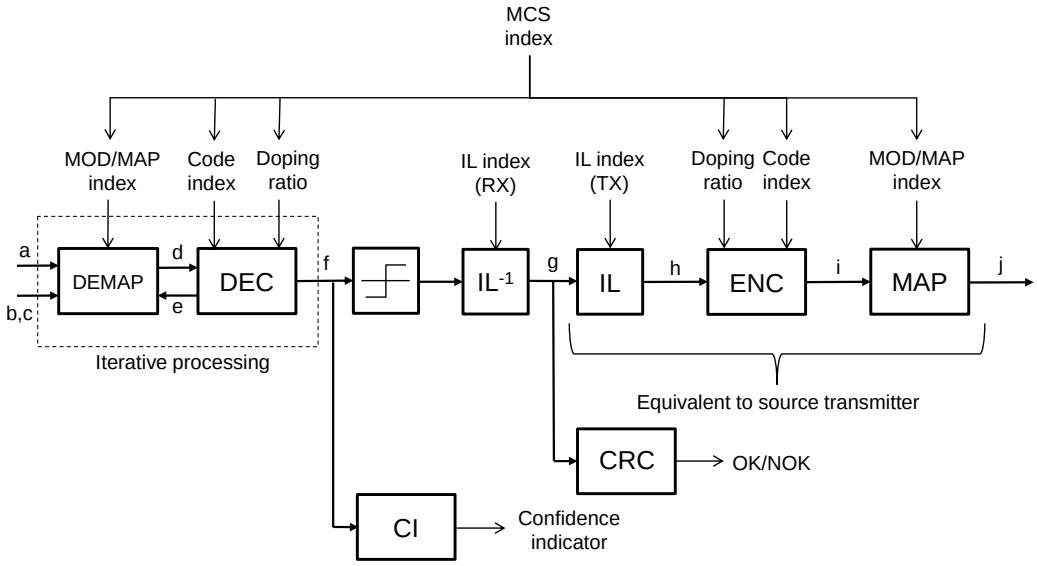

Figure 5.2: Block diagram of the relay functionality.

5.2.2 Simulation Abstraction for Higher Layers

In the system level, and for the higher layer functionalities such as multi-rate control, power control, ARQ, and MAC, it is desirable to be able to run simulations without the need to implement all the details of the physical layer. For cellular systems, it is a common practice to apply link quality metric tools such as Exponential Effective SNR Mapping (EESM) or Mutual Information (MI) based mapping [TS03; WTA06; YZW+14]. In essence, based on the knowledge of the SNR level, and the (time or frequency selective) fading channel coefficients, the metric attempts to describe the link quality with just one scalar parameter that is the effective SINR or MI. The total MI is the average of the MIs per subchannel, and the assumption is that at certain averaged MI level, the decoding performance is the same regardless of how MI is divided into subchannels. The MI metric itself is independent of the FEC coding scheme, but can be formulated as dependent on the modulation constellation such as QPSK and 16QAM. The metric can be used

- in simulations, to predict or approximate the block error probability (BLER) without running the actual coding and decoding processes, or
- in multi-rate control, to choose the appropriate modulation and coding parameters.

In order to create the mapping from SINR or MI to BLER, coding and decoding simulations are usually run for example in the AWGN channel. Thus, code design and decoder implementation dependent performance mapping is obtained. Each modulation and coding scheme as well as code block length may be simulated separately in order to get an accurate mapping.

The MI-based metric suits well the RESCUE system model where multiple parallel links with the same data are received. However, a RESCUE-specific problem remains: how to deal with the decoding errors at relay transmitters. To address this issue, one can employ the information theoretic outage probability analysis derived for the case of single-relay lossy forwarding in [ZCH+14]. The analysis is based on the theory of source coding with side information.

WP2 proposes to create a quality mapping that predicts the BER distribution at a receiver that combines multiple packet copies. The purpose is to facilitate fast and flexible simulations of the higher layers in terms of multi-rate control, power control, ARQ, and MAC.

A simplified version of the "admissible rate region" from [ZCH+14] is shown in Figure 5.3. The figure corresponds to a three-node system model, where the destination receives two copies of the same data packet, one directly from the source and another from a relay node. Here, the relay is unable to decode correctly, and the resulting BER at the relay is p. The axes R_1 and R_2 represent the normalized channel constellation constrained capacities (mutual information) of the source-to-destination link and the relay-to-destination link, respectively. Theoretically, if the rate pair falls into the admissible rate region, error-free decoding at the destination is possible. Note that the rate region is information theoretic and independent of the code design and decoder implementation. We can assume that the source data has full entropy, i.e., $H(U_1) = 1$, and that the data transmitted by the relay also has full entropy so that $H(U_2) = 1$.

The bound of the admissible rate region consists of the straight line a

$$R_1 + (1 - H_b(p_i)) = 1 \tag{5.1}$$

and the curve b. In order to simplify the model, we approximate the curve by the straight c as

$$R_1 + (1 - H_b(p_i))\,R_2 = 1. \tag{5.2}$$

By combining the two lines, we get an expression for the approximated admissible rate region as

$$R_1 + \min\{1 - H_b(p_i), (1 - H_b(p_i))R_2\} \geq 1 \tag{5.3}$$

We further propose to generalize the combining of MI over any number of parallel incoming links so that

$$M = \sum_i M_i \tag{5.4}$$

$$M_i = \begin{cases} R_i, & p_i = 0 \\ \min\{(1 - H_b(p_i))R_i, 1 - H_b(p_i)\}, & p_i > 0 \end{cases} \tag{5.5}$$

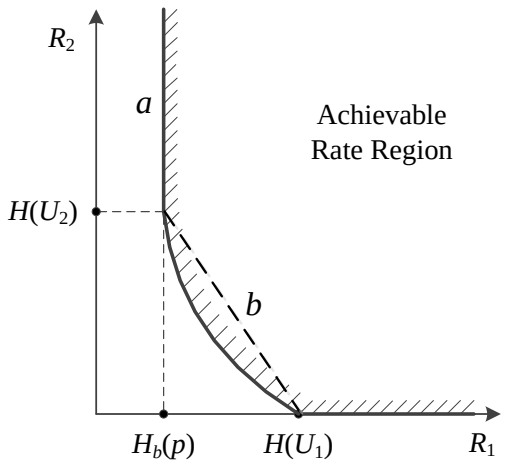

Figure 5.3: Rate region for black boxes.

In theory, when MI per bit is unity, it is perfect. Note that if there are errors in the transmitter, corresponding MI remains always below unity. Otherwise, MI can get larger values.

By employing the Shannon's source-channel separation theorem, the distortion (BER) at the output of the receiver can be lower bounded by the inverse of the binary entropy function [ZCH+14] as

$$p_e = H_b^{-1}(1-M), \tag{5.6}$$

which equals to zero when $M \geq 1$. We call the mapping from the link-specific SNRs and transmitter BERs into the MI and receiver BER as "black box #1" as shown in Figure 5.4. It employs a very simple deterministic mapping that is independent of the coding and decoding scheme, and requires no simulations. It predicts optimistic performance that corresponds to infinite packet sizes and perfect codes.

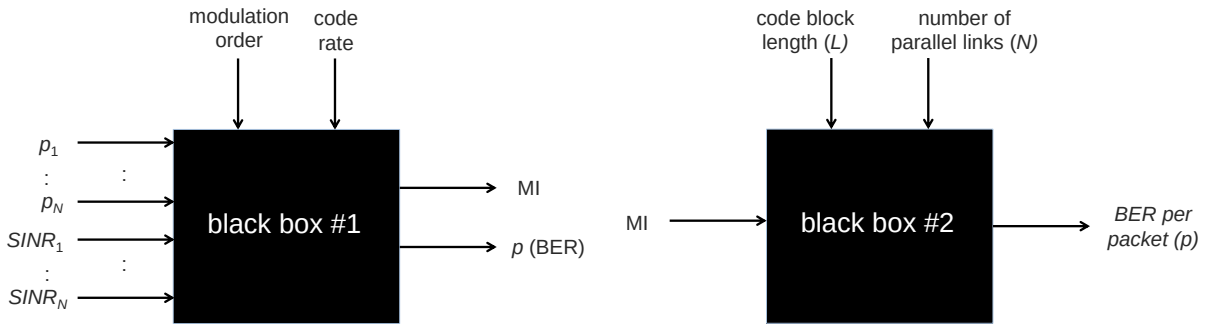

Figure 5.4: Black boxes 1 and 2.

In order to obtain code, decoder, and packet length dependent BER performance results, we propose to concatenate black box #1 with black box #2 that employs a mapping obtained via simulations in the AWGN channel. The idea is to obtain the random packet-by-packet decoding performance in terms BER.

The composite black box model is capable of providing BER performance per simulated packet, which depends on the code rate and the SNRs of the parallel links. The black box model shall be used by WP3 to characterize the performance of their proposed MAC, ARQ, and routing protocols, based on the simulated BER.

6. Conclusion

This deliverable provided initial results and descriptions of the coding/decoding and source-correlation estimation algorithms considered in the RESCUE project. First, the state-of-the-art in the case of a simple network model consisting of a single source, a set of parallel relay nodes, and one destination node was summarized. Then, new source-correlation estimation methods and signaling protocols that aim to improve the joint decoding performance or to reduce the estimation complexity were proposed. Furthermore, more general system models were considered, including non-orthogonal multiple access for the relay transmissions, multi-hop networks where the destination is more than two hops away from the source, and multiple-access relaying where two sources utilize a single relay node. Finally, a preliminary description of the new simulation abstraction concept, called ”black box”, that aims to support system level development and simulations, was given. Also, some code design choices for the SDR implementation and demonstration were discussed.

For the simple ”toy scenarios” addressed in Chapter 2, no major performance improvements by code design can be found since the performance of the state-of-the-art codes is already close to the theoretical limit. The remaining challenge and the main novel contribution of this deliverable lie in more practical aspects: how to estimate or signal the correlation between the relayed data sequences to the destination. Several novel ideas concerning this problem were proposed in Chapter 3. In the usual scenario where the data packets are accompanied by CRC fields, it makes sense for the relays to check it, and to signal the result to the destination along with the forwarded data. Similarly, it is beneficial for the destination to know if one of the transmitters is actually the source: this way the joint decoder can rely on hard facts about the transmitted sequence. However, when the CRC check fails at the relay, more refined estimates of the BER of the decoded data packet can be obtained by estimating the SNR of the incoming channel, or by calculating the confidence indicator (CI) based on the post-decoding LLRs. Finally, as estimates are always in practice inaccurate, the estimates provided by the relays could be further improved by utilizing pairwise BER estimation methods at the destination in conjunction with the iterative decoder. It is certainly a future design challenge to find a protocol that provides the best trade-off between decoding performance, estimation complexity, and signaling overhead.

When the network model is extended to cover more than two hops between the source and the relay, the multi-route coding and decoding problem gets more challenging. For example, the decoding strategy at the relays needs to be selected. If complexity is not an issue, the relays may carry out the same type iterative multi-packet combining as the destination does. On the other hand, at the destination, the errors in the received packet copies may become correlated, when the same errors are transmitted by the parallel relays of the second stage. However, as shown in Section 4.2, the cross-link problem does not seem to be severe, at least when the error probabilities remain relatively low. Multi-hop relaying and more general topologies as well as communication scenarios are in the central focus of WP2 in the near future.

So far, WP2 has evaluated the performance in simplified models only, and mainly in terms of BER/FER as a function of link-level SNRs. This approach is not completely fair in terms of the total transmit energy consumption and spectral efficiency. It is recognized that the multi-route coding gain needs to compensate for the bandwidth expansion caused by the parallel relays that reserve orthogonal time slots. One efficient way of avoiding the bandwidth expansion is IDMA, where the relays are allowed to transmit at the same time in a non-orthogonal manner. IDMA is studied in more details in WP1. Finally, the real test of the links-on-the-fly concept is carried out when system level protocols such as ARQ and MAC are integrated with the coding strategy. The preliminary descriptions of the higher layer protocols will be disclosed in another RESCUE deliverable D3.1 [D31].

7. References

[AM12a] Khoirul Anwar and Tad Matsumoto. "Accumulator-assisted distributed Turbo codes for relay systems exploiting source-relay correlation". In: *IEEE Commun. Lett.* 16.7 (July 2012), pp. 1114–1117.

[AM12b] Khoirul Anwar and Tad Matsumoto. "Spatially Concatenated Codes with Turbo Equalization for Correlated Sources". In: *IEEE Trans. Signal Processing* 60.10 (Oct. 2012), pp. 5572–5577.

[BK04] Maria L. Blanton and James J. Kaput. "Instructional Contexts That Support Students' Transition From Arithmetic to Algebraic Reasoning: Elements of Tasks and Culture". In: *Everyday Matters in Science and Mathematics: Studies of Complex Classroom Events*. Ed. by Ricardo Nemirowsky, Ann S. Rosebery, Jesse Solomon, and Beth Warren. Routledge, 2004. Chap. 7, pp. 211–234.

[Bri01] S. ten Brink. "Convergence behavior of iteratively decoded parallel concatenated codes". In: *IEEE Trans. Commun.* 49.10 (Oct. 2001), pp. 1727–1737.

[BS05] H. Behroozi and M.R. Soleymani. "Performance of the successive coding strategy in the CEO problem". In: *Proc. IEEE Global Telecommun. Conf., 2005.* Vol. 3. Nov. 2005, pp. 1347–1352.

[BS09] Hamid Behroozi and M.R. Soleymani. "Optimal rate allocation in successively structured Gaussian CEO problem". In: *IEEE Trans. Wireless Commun.* 8.2 (Feb. 2009), pp. 627–632.

[BZV96] Toby Berger, Zhen Zhang, and Harish Viswanathan. "The CEO problem [multiterminal source coding]". In: *Information Theory, IEEE Transactions on* 42.3 (1996), pp. 887–902.

[CBV05] R. Cristescu, B. Beferull-Lozano, and M. Vetterli. "Networked Slepian-Wolf: theory, algorithms, and scaling laws". In: *IEEE Trans. Inform. Theory* 51.12 (Dec. 2005), pp. 4057–4073.

[CCC00] Won-Joon Choi, Kok-Wui Cheong, and J.M. Cioffi. "Iterative soft interference cancellation for multiple antenna systems". In: *Wireless Communications and Networking Confernce, 2000. WCNC. 2000 IEEE*. Vol. 1. 2000, 304–309 vol.1.

[CIA+12] Meng Cheng, Ade Irawan, Khoirul Anwar, and Tad Matsumoto. "BICM-ID for Relay System Allowing Intra-link Errors and a Similarity Constellation to ARQ Schemes". In: *Progress in Electromagnetics Research Symposium (PIERS)*. Kuala Lumpur, Malaysia, Mar. 2012, pp. 281–286.

[CP07] Donghui Chen and Robert J. Plemmons. "Nonnegativity constraints in numerical analysis". In: *Symposium on the Birth of Numerical Analysis*. Leuven Belgium, Oct. 2007.

[CZA+12] M. Cheng, X. Zhou, K. Anwar, and T. Matsumoto. "Simple Relay Systems with BICM-ID Allowing Intra-Link Errors". In: *IEICE Trans. on Commun.* E95-B.12 (Dec. 2012), pp. 3671–3678.

[D11] ICT-619555 RESCUE Deliverable. *D1.1 – System Scenarios and Technical Requirements*. Tech. rep. May 2014.

[D31] ICT-619555 RESCUE Deliverable. *D3.1 – MAC and Routing Architecture and Interfaces Specification*. Tech. rep. Nov. 2014.

[FOO00] P. Frenger, P. Orten, and T. Ottosson. "Code-spread CDMA using maximum free distance low-rate convolutional codes". In: *IEEE Trans. Commun.* 48.1 (Jan. 2000), pp. 135–144.

[FOT+12] K. Fukawa, S. Ormsub, A. Tölli, K. Anwar, and T. Matsumoto. "EXIT-constrained BICM-ID Design using Extended Mapping". In: *EURASIP Journal on Wireless Commun. and Networking* 2012. 1 (Feb. 2012).

[GK11] A.E. Gamal and Y.H. Kim. *Network Information Theory*. Cambridge University Press, 2011.

[GZ05] Javier Garcia-Frias and Ying Zhao. "Near-Shannon/Slepian-Wolf performance for unknown correlated sources over AWGN channels". In: *IEEE Trans. Commun.* 53.4 (2005), pp. 555–559.

[HBP08] J. Haghighat, Hamid Behroozi, and D.V. Plant. "Iterative joint decoding for sensor networks with binary CEO model". In: *Proc. IEEE Works. on Sign. Proc. Adv. in Wirel. Comms., 2008.* July 2008, pp. 41–45.

[HOP96] J. Hagenauer, E. Offer, and L. Papke. "Iterative decoding of binary block and convolutional codes". In: *IEEE Trans. Inf. Theory,* 42.2 (Mar. 1996), pp. 429–445.

[HZA+13] Xin He, Xiaobo Zhou, Khoirul Anwar, and Tad Matsumoto. "Estimation of Observation Error Probability in Wireless Sensor Networks". In: *IEEE Commun. Lett.* 17.6 (June 2013), pp. 1073–1076.

[HZJ+14] Xin He, Xiaobo Zhou, Markku Juntti, and Tad Matsumoto. "Data and Error Rate Bounds for Binary Data Gathering Wireless Sensor Networks". In: *submitted to IEEE Trans. Wireless Commun.* (2014).

[IH11] O. Iscan and C. Hausl. “Iterative Network and Channel Decoding for the Relay Channel with Multiple Sources”. In: *2011 IEEE Vehicular Technology Conference (VTC Fall)*. Sept. 2011, pp. 1–5.

[LTA+11] Pen-Shun Lu, V. Tervo, K. Anwar, and T. Matsumoto. “Low-Complexity Strategies for Multiple Access Relaying”. In: *IEEE 73rd Vehicular Technology Conference (VTC Spring)*. Budapest, Hungary, May 2011, pp. 1–6.

[LVW+06] Yonghui Li, B. Vucetic, T.F. Wong, and M. Dohler. “Distributed Turbo Coding With Soft Information Relaying in Multihop Relay Networks”. In: *IEEE J. Select. Areas Commun.* 24.11 (2006), pp. 2040–2050.

[LZM14] Pen-Shun Lu, Xiaobo Zhou, and Tad Matsumoto. “Outage Probabilities of Orthogonal Multiple-Access Relaying Techniques with Imperfect Source-Relay Links”. In: *submitted to IEEE Trans. Wireless Commun.* (2014).

[Ooh98] Yasutada Oohama. “The rate-distortion function for the quadratic Gaussian CEO problem”. In: *IEEE Trans. Inform. Theory* 44.3 (May 1998), pp. 1057–1070.

[RA12] A. Razi and A. Abedi. “Adaptive bi-modal decoder for binary source estimation with two observers”. In: *2012 46th Annual Conference on Information Sciences and Systems (CISS)*. Mar. 2012, pp. 1–5.

[RYA11] A. Razi, K. Yasami, and A. Abedi. “On minimum number of wireless sensors required for reliable binary source estimation”. In: *Proc. IEEE Wireless Commun. and Networking Conf.* Mexico, Mar. 2011, pp. 1852–1857.

[SIT10] K. Sakakibara, D. Ito, and J. Taketsugu. “Outage probability of cooperative multi-hop relay networks with MDS codes at link-level”. In: *Electronics and Telecommunications (ISETC), 2010 9th International Symposium on*. Nov. 2010, pp. 141–144.

[SLW+09] Gang Shen, Jimin Liu, Dongyao Wang, Jikang Wang, and Shan Jin. “Multi-hop relay for next-generation wireless access networks”. In: *Bell Labs Technical Journal* 13.4 (2009), pp. 175–193.

[SW73] D. Slepian and J. Wolf. “Noiseless coding of correlated information sources”. In: *IEEE Trans. Inform. Theory* 19.4 (July 1973), pp. 471–480.

[Tho08] R. Thobaben. “On distributed codes with noisy relays”. In: *42nd Asilomar Conference on Signals, Systems and Computers*. Pacific Grove, CA, Oct. 2008.

[TS03] S. S. Tsai and A. C. K. Soong. *Effective-SNR Mapping for Modeling Frame Error Rates in Multiple-state Channels*. 3GPP2-C30-20030429-010, Ericsson, 3rd Generation Partnership Project 2 (3GPP2). 2003.

[VB97] H. Viswanathan and T. Berger. “The quadratic Gaussian CEO problem”. In: *IEEE Trans. Inform. Theory* 43.5 (Sept. 1997), pp. 1549–1559.

[VS99] S. Verdu and S. Shamai. “Spectral efficiency of CDMA with random spreading”. In: *IEEE Trans. Inform. Theory* 45.2 (Mar. 1999), pp. 622–640.

[WAM14] Kun Wu, Khoirul Anwar, and Tad Matsumoto. “BICM-ID-Based IDMA: Convergence and Rate Region Analyses”. In: *IEICE Trans. on Commun.* E97-B.7 (July 2014), pp. 1483–1492.

[WTA06] Lei Wan, Shiauhe Tsai, and Magnus Almgren. “A Fading-Insensitive Performance Metric for a Unified Link Quality Model”. In: *Proc. IEEE Wireless Commun. and Networking Conf.* Vol. 4. Apr. 2006, pp. 2110–2114.

[YG11] Roua Youssef and Alexandre Graell i Amat. “Distributed Serially Concatenated Codes for Multi-source Cooperative Relay Networks”. In: *IEEE Trans. on Wireless Communications* 10.1 (Jan. 2011), pp. 253–263.

[YLR+12] Qimin You, Yonghui Li, M.S. Rahman, and Zhuo Chen. “A near optimal routing scheme for multi-hop relay networks based on Viterbi algorithm”. In: *IEEE International Conference on Communications (ICC)*. June 2012, pp. 4531–4536.

[YZW+14] Juwo Yang, Hui Zhao, Wenbo Wang, and Chengcheng Zhang. “An Effective SINR Mapping Models for 256QAM in LTE-Advanced System”. In: *IEEE International Symposium on Personal Indoor and Mobile Radio Communications (PIMRC)*. Washington D.C., USA, Sept. 2014.

[ZCA+12] Xiaobo Zhou, Meng Cheng, Khoirul Anwar, and Tad Matsumoto. “Distributed joint source-channel coding for relay systems exploiting source-relay correlation and source memory”. In: *EURASIP Journal on Wireless Communications and Networking* 2012:260 (2012).

[ZCH+14] Xiaobo Zhou, Meng Cheng, Xin He, and Tad Matsumoto. “Exact and Approximated Outage Probability Analyses for Decode-and-Forward Relaying System Allowing Intra-link Errors”. In: *IEEE Trans. Wireless Commun.* ((Accepted) 2014).

[ZHA+12] Xiaobo Zhou, Xin He, Khoirul Anwar, and Tad Matsumoto. “GREAT-CEO: larGe scale distRibuted dEcision mAking Techniques for Wireless Chief Executive Officer Problems”. In: *IEICE Trans. on Comm., Special Section on Coding and Coding Theory-Based Signal Processing for Wireless Communications* E95-B.12 (2012), pp. 3654–3662.